UNIVERSIDADE DE LISBOA
FACULDADE DE CIÊNCIAS
DEPARTAMENTO DE BIOLOGIA ANIMAL

The role of microRNAs in Haematopoiesis and Immunity of *Drosophila melanogaster*

Mestrado em Biologia Evolutiva e do Desenvolvimento

Joana Gomes Campos de Carvalho

Dissertação orientada por:
Élio Sucena
(Faculdade de Ciências da Universidade de Lisboa e Instituto Gulbenkian de Ciência)

2016

Acknowledgements

Reaching the end of my first step in the big world of academic research was no easy task and being surrounded by amazing people throughout the process is highly advised and helps you to be amazing too. To everyone who contributed to this achievement, thank you.

I want to thank everyone from the groups of Élio Sucena, Patrícia Beldade and Christen Mirth from the EvoDevo community at Instituto Gulbenkian de Ciência. They created the best possible working environment and source of healthy motivation and constructive criticism one could ask for.

I thank Élio Sucena for trusting me since the beginning and giving me the creative freedom others can only dream of. Thank you for being such an inspiration and keeping me in the right track.

I want to thank Julien Marcetteau, the most talented and kind friend, who was essential for the success of this project and without whom it would not exist.

I also thank Tânia and Nuno, for the important experimental guidelines throughout the project, and the remaining of my friends who directly or indirectly contributed to the important comical reliefs of the story.

Finally, I want to thank my sisters and mother, who were strong enough to endure in the best and worst moments of my progress, and my all-time companion who gave me such valuable creative input and important life lessons without ever leaving my side.

Resumo em Português

A resposta imune de *Drosophila melanogaster* envolve múltiplas estratégias de defesa que são relativamente conservadas entre animais. De forma geral, esta resposta resulta da interacção entre uma componente humoral, também designada por imunidade sistémica, e uma componente celular, que implica a diferenciação de vários tipos de células especializadas.

A imunidade sistémica consiste na produção de péptidos antimicrobianos (PAMs) pelas células do corpo adiposo e de componentes das reacções de melanização e de stress oxidativo que actuam no sentido de neutralizar patogéneos. Os PAMs acumulam-se na hemolinfa e a sua produção ocorre principalmente através das vias de sinalização Toll e Immune defficiency (Imd), que são activadas após o reconhecimento de certos componentes da parede celular de bactérias gram-positivas ou fungos e bactérias gram-negativas, respectivamente. Além disso, existem outras vias de sinalização que tembém podem participar na resposta humoral. A via JNK (JUN N-terminal kinase) é activada por componentes da via Imd e tem um papel importante na indução de apoptose e na remodelação do citoesqueleto e adesão das células. Além disso, está envolvida na resistência ao stress oxidativo. A via JAK-STAT, por sua vez, está relacionada com a resposta à infecção viral e com a produção de citocinas e factores de resposta ao stress. Embora a existência de diferentes cascatas de sinalização confira especificidade à resposta imune, certos tipos de infecção podem levar a uma activação sinergística das mesmas vias. As lesões sépticas (picada com uma agulha embebida em solução bacteriana), por exemplo, activam tanto a via Toll como a via Imd, levando à produção de PAMs como a *Diptericina* e a *Drosomicina*.

A componente celular da resposta imune de *D. melanogaster* tem como intervenientes principais os hemócitos (células do sangue), que são descritos como funcionalmente análogos à linhagem mielóide dos vertebrados. Em homeostase, 90% dos hemócitos são plasmatócitos, que têm capacidade fagocítica e contribuem para a activação da produção de PAMs, e 10% são células cristal, que participam nas reacções de melanização e na regeneração de feridas. Além disso, mediante a ocorrência de uma ferida ou de endoparasitismo, há diferenciação de lamelócitos sob o controlo da via JAK-STAT, que são importantes para a encapsulação de microorganismos de maiores dimensões. Os efectores da componente celular da resposta imune são gerados e mantidos através do processo de desenvolvimento designado de hematopoiese, que ocorre ao longo do ciclo de vida em diferentes compartimentos. Nos estadios larvares, onde este processo é mais activo, a glândula linfática é o principal orgão hematopoiético em que células progenitoras dão origem a plasmatócitos e células cristal. Fora deste órgão, existem hemócitos em circulação e em agregados sésseis na epiderme dorsal ao longo dos segmentos corporais. Nestes tecidos existe também proliferação e diferenciação de hemócitos, que se encontram em equilíbrio dinâmico com o compartimento circulatório. Embora a exacta contribuição de cada uma das componentes da resposta imune ainda não esteja bem estabelecida, a sua acção combinada pensa-se que seja importante para a neutralização e eliminação de microorganismos invasores.

Os microRNAs (miRNAs), classificados como sequências curtas e não codificantes que actuam através do silenciamento da expressão génica, têm vindo a emergir como reguladores de muitos programas de desenvolvimento animal e de muitas respostas biológicas, incluindo a resposta imune. Enquanto nos vertebrados o repertório de funções descritas para os miRNAs inclui tanto a regulação da diferenciação e proliferação celular durante a hematopoiese, como a produção de anticorpos e citocinas, nos invertebrados, e particularmente em *D. melanogaster*, a informação relativa à função dos miRNAs torna-se relativamente escassa.

Este projecto pretende abordar esta questão e dissecar o papel destas sequências no sistema

imune de *D. melanogaster,* através de *screens* sistemáticos que englobam a maioria dos microRNAs presentes no genoma deste organismo modelo. Incidindo tanto no processo de hematopoiese larvar, que dá origem aos efectores da componente celular, como na resposta imune sistémica dos adultos, cuja função influencia a resistência à infecção bacteriana, os nossos resultados indicam que vários miRNAs têm papéis regulatórios importantes nestas duas vertentes da resposta imune.

Os resultados obtidos através de infecção sistémica com *Pseudomonas entomophila* e *Pseudomonas putida,* duas bactérias do tipo gram-negativo, mostram que as delecções dos mir-317 e mir-137 aumentam a susceptibilidade à infecção bacteriana, causando taxas de mortalidade elevadas. Por outro lado, a delecção do cluster mir-100/let-7/mir-125 revela uma redução da mortalidade no contexto de infecção, provavelmente relacionada com uma maior resistência ou tolerância à infecção com bactérias gram-negativas. Apesar de apresentarem dinâmicas opostas entre as duas bactérias testadas, também as delecções do mir-31b e do mir-2b-1 apresentam diferenças significativas na susceptibilidade à infecção bacteriana. De acordo com as previsões bioinformáticas, os alvos destas sequências incluem vários componentes da resposta imune sistémica, nomeadamente proteínas das vias Imd e Toll, assim como componentes importantes para a regulação da resposta de stress oxidativo. Além disso, estes miRNAs têm como alvos proteínas importantes para a fisiologia geral do organismo, que também podem impactar a sobrevivência após infecção bacteriana.

Por sua vez, os miRNAs também desempenham funções importantes na hematopoiese em *D. melanogaster*, particularmente no que toca à adesão e diferenciação de vários tipos de hemócitos. Os nossos resultados indicam que as delecções do mir-969 e do mir-124 causam aumento e diminuição da densidade de plasmatócitos nos agregados sésseis, respetivamente. Isto tem consequências para os números de células cristal, que dependem do correcto estabelecimento da densidade de plasmatócitos, já que estas se transdiferenciam a partir dos mesmos. Estas duas sequências de miRNAs têm como alvos genes importantes para a adesão e migração celular, processos estes que podem influenciar a densidade de plasmatócitos nos órgãos hematopoiéticos de *D. melanogaster*. A delecção do mir-1 em heterozigotia, por sua vez, revelou um decréscimo significativo na densidade de células cristal, indicando que este miRNA tem um papel importante na regulação da transdiferenciação deste tipo celular, processo este que é mediado pela sinalização Notch. A previsão bioinformática dos alvos desta sequência revela que o mir-1 inclui vários componentes da via de sinalização Notch, reforçando a ideia de que poderá regular o processo de diferenciação de células cristal. Finalmente, a delecção do mir-980 causa uma redução acentuada nos números de plasmatócitos e células cristal, levando a uma disrupção da estrutura e integridade dos tecidos hematopoiéticos larvares. Isto deve-se a uma diferenciação ectópica de lamelócitos, que entram em circulação e levam à formação de tumores melanóticos, como resultado da encapsulação exacerbada dos própios tecidos. A análise in silico dos alvos do mir-980 revelou que o mRNA de *domeless*, que codifica para o receptor da via JAK-STAT, interage fortemente com o mir-980. Uma vez disrompido o mecanismo de silenciamento deste gene, por via da delecção do mir-980, a sobreexpressão de Domeless poderá levar à activação da via JAK-STAT e consequentemente à diferenciação exacerbada de lamelócitos. Resultados preliminares revelam que a remoção do mir-980 causa uma mudança no padrão de activação da via JAK-STAT, possivelmente em tecidos como o corpo adiposo ou os músculos somáticos e uma pequena percentagem de hemócitos.

No futuro, a análise detalhada da origem dos vários fenótipos observados permitirá a caracterização e compreensão do impacto deste mecanismo de regulação na resposta imune de *D. melanogaster.* Particularmente, será importante analisar o tempo e local de expressão dos miRNAs candidatos e os seus alvos, assim como a nessecidade e a suficiência de cada uma destas sequências para regulação dos vários mecanismos que contribuem para a resposta imune de *D. melanogaster*.

Palavras-chave

Hematopoiese; Imunidade; microRNAs; *D. melanogaster*

English Summary

The immune response of *Drosophila melanogaster* involves multiple innate defences that are conserved in higher organisms and have been largely characterized. Consisting of an interaction between a humoral and a cellular component, it is essential for the neutralization and elimination of invading microorganisms. While the humoral defences refer mainly to the production of antimicrobial peptides (AMPs), cellular defences include different haemocyte-mediated responses like phagocytosis, melanization and encapsulation. MicroRNAs, short non-coding sequences that silence gene expression, are emerging as regulators of several developmental programs and biological responses, including the immune response. Furthermore, they have been implicated in processes like antibody switching and lineage determination in mammalian haematopoiesis or regulation of AMP levels in *D. melanogaster*. Here we proposed to dissect the role of these sequences in the immune system of *D. melanogaster* by performing a systematic loss-of-function screen that covers the majority of microRNAs present in its genome. Focusing on both the larval haematopoiesis and the adult systemic response, we have revealed a set of candidate microRNAs that are important for the regulation of resistance to bacterial infection and haemocyte differentiation. Our results indicate mir-317 and mir-137 loss-of-functions dramatically increase susceptibility to bacterial infection by *Pseudomonas entomophila* and *Pseudomonas putida*, leading to high mortality rates. On the other hand, the mir-100/let-7/mir-125 cluster knock-out shows a significant decrease in mortality, related to higher resistance or tolerance to gram-negative bacterial infection. Furthermore, we have shown that mir-124 and mir-969 impact plasmatocyte adhesion, influencing the density of cells in the sessile haemocyte clusters of larvae. Deletion of mir-1 is important for the regulation of the differentiation of crystal cells, which are mainly involved in melanization and wound healing. Finally, we have shown that mir-980 loss-of-function causes ectopic lamellocyte differentiation, a cryptic cell type that is crucial for the encapsulation mechanism and normally triggered upon parasitoid wasp infection. *In silico* predictions have revealed that these candidates can directly target immune-related genes and modulate their expression levels. Further investigation will allow us to provide a better understanding of the impact of these microRNAs on their corresponding targets and the immune response pathways that include them.

Key-Words

Haematopoiesis; Immunity; microRNAs; *D. melanogaster*

Table of Contents

1. Introduction

The interactions between multicellular organisms and pathogens have long shaped the evolution of the immune system. Innate immunity, which consists in a first-line defense against pathogenic challenges, is likely to be common to all metazoans[1]. Insects, for instance, rely solemnly on innate defences to mount a complex and multifaceted immune response[2]. *Drosophila melanogaster,* widely used as a model to study innate immunity[3], breed, lay eggs and develop in decomposing media, being constantly exposed to a wide variety of pathogens. Once such pathogens cross the epithelial barriers and enter the body cavity (haemocoel) both cellular and humoral defences are mobilized (Figure 1.1). While the digestive tract is the main contributor to haemocoel microbial load, septic injury and endoparasitism can also induce pathogenicity and shape immune response evolution[3].

1.1 The immune response of *Drosophila melanogaster*

The immune response of *D. melanogaster* consists of an interaction between a humoral component known as the systemic immune response and a cellular component, the latter involving the differentiation of several specialized cell types[2] (Figure 1.1). The systemic immune response consists of a coordinated activation of proteolytic cascades and production of melanization and oxidative stress components that neutralize invading pathogens[2]. The hallmark of this process is the systemic antimicrobial response, the challenge induced synthesis and secretion of antimicrobial peptides (AMPs) by the fat body[4]. AMPs accumulate in the circulating haemolymph and have a distinct yet overlapping specificity, targeting fungi, gram-positive and gram-negative bacteria[5]. The production of AMPs involves two main pathways: Toll and Immune deficiency (Imd), both intracellular cascades that are activated when conserved components of the microbial cell wall are detected by and bound to recognition proteins[2].

Gram-positive bacteria and fungi are recognized by both peptidoglycan-recognition proteins (PGRPs) and gram-negative binding proteins (GNBPs), preferentially activating the Toll pathway. Activation of the Toll pathway occurs after cleavage of the recognition complex, when the cytokine Spätzle binds to the extracellular region of the Toll receptor[6]. Such binding triggers conformational changes in the receptor that activate the intracellular signalling cascade. Once Toll signalling is induced, a pre-signalling complex is assembled, consisting of MyD88, Tube and Pelle, that leads to phosphorylation and degradation of Cactus. The result is the graded release and nuclear translocation of Dif (Dorsal-related immunity factor), a nuclear factor κB (NF-κB), which induces the expression of AMP genes such as *Drosomycin*[4]. Gram-negative bacteria recognition is achieved through the sensing of specific forms of peptidoglycan by PGRPs, which will mainly activate the Imd pathway[4,5]. After peptidoglycan components of the microbial cell wall are recognized by transmembrane PGRPs, the IMD adaptor mediates the action of the intracellular domains of PGRPs functioning as a signalling platform. One of its targets is the NF-κB-like transcription factor Relish[4], which is cleaved by at least three proteins: Imd, the adaptor Fadd (FAS-associated death domain) and the caspase Dredd (death-related ced-3/Nedd2- like protein)[7]. After cleavage, the Rel domain translocates to the nucleus and, as the Toll pathway effector Dif, binds to κB binding sites on the promoter of target genes[2] which include the AMP *Diptericin*, a common read-out of Imd pathway activation[4].

In addition to initiating Relish signalling, immune stimulation of the Imd pathway also activates the JUN N-terminal kinase (JNK) pathway. The branch point between the two signalling cascades is thought to occur upstream of the cleavage of Relish, mediated by TAK1[8]. The JNK pathway is known to control the expression of a cluster of immune-dependent genes that include proteins involved in cytoskeleton remodeling, cell adhesion and apoptosis induction[2,9]. Importantly,

JNK signalling is involved in resistance to oxidative stress and may briefly control the expression of some AMP genes[10].

Finally, another pathway implicated in the humoral response of *D. melanogaster* is the JAK-STAT signalling pathway. This includes the response against viral infection and the production of immune-related cytokines and stress response factors[11]. In fact, JAK/STAT is activated in response to secreted Unpaired cytokines (Upd, Upd2, Upd3). Extracellular binding to the receptor Domeless induces a conformational change that triggers the intracellular phosphorylation of the janus kinase signal transductor (JAK), Hopscotch. This reaction allows the creation of docking sites for the phosphorylation of members of the STAT family of transcription factors, which in turn can translocate to the nucleus and activate the transcription of several target genes[11].

The existence of different pathways and recognition molecules confers specificity to the immune response of *Drosophila*. However, some challenges can lead to the synergistic activation of several pathways. Septic injuries (pricking with a bacteria-soaked needle), for instance, strongly activate the Toll pathway and expression of *Drosomycin*, while transiently inducing *Diptericin* production through the Imd pathway. Furthermore, production of *Drosomycin*, the best described anti-fungal peptide, depends on the type of immune response that is triggered, being produced by both pathways in the case of the systemic response or just by one of them (Toll) in the case of the local one[2,13].

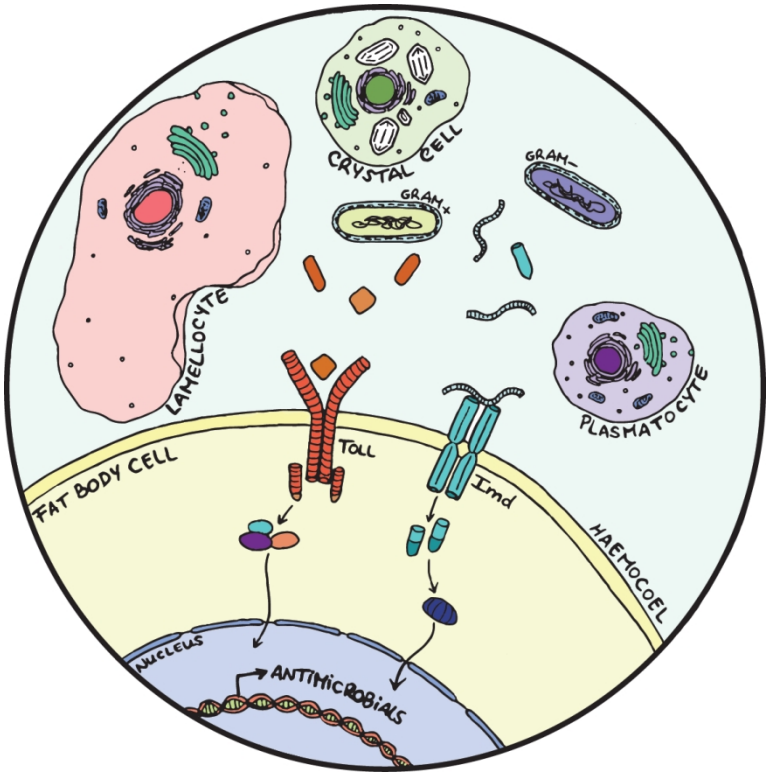

Figure 1.1 – The humoral and cellular components of the immune response of *Drosophila melanogaster*. Humoral defences include the activation in the fat body cells of Toll and Imd, intracellular signalling cascades that are responsible for the production of antimicrobial peptides (AMPs). Cellular defences include phagocytosis and melanization which are guaranteed, respectively, by plasmatocytes and crystal cells. Upon injury or parasitoid wasp infection lamellocytes are differentiated, mainly participating in the encapsulation reaction.

The immune response of *D. melanogaster* further includes a cellular component that acts in parallel with the humoral defences towards a more generalized capacity to efficiently cope with infection. The main effectors here are the haemocytes (blood cells), usually described as functionally analogous to the vertebrate myeloid lineage[14]. Based on their structural and functional features, haemocytes are divided into three cell types: plasmatocytes, crystal cells and lamellocytes.

Plasmatocytes display phagocytic activity, mainly taking up apoptosis debris, particularly throughout development. Additionally, they are important for the phagocytosis of bacteria and contribute to the activation of AMP production[15]. Crystal cells are characterized by large prophenoloxidase (PPO) inclusions and are involved in melanization and wound healing, by rupturing and releasing PPO into the haemolymph under the control of the JNK pathway[16]. Lamellocytes are large cells generated only in response to specific immune challenges and are essential for the encapsulation of microorganisms too large to be engulfed exclusively by plasmatocytes[2,17].

These effectors of the cellular immune response are generated and maintained through the developmental process of haematopoiesis. In *Drosophila*, it is established to occur during two developmental stages, embryonic and larval, in spatially separated compartments[2]. The first wave of haematopoiesis takes place during embryogenesis, when cells of the head mesoderm of early embryos give rise to plasmatocytes and crystal cells that persist throughout larval development and into adulthood[18]. The second wave of haematopoiesis occurs in the larval stages of development and is characterized by the expansion of the existing embryonic haemocytes and by differentiation within the larval haematopoietic organ, the lymph gland (LG)[19]. Different compartments contribute to the maintenance and expansion of these cellular populations[20]. The LG is a specialized organ located in the anterior end of the dorsal vessel that differentiates and disintegrates upon pupation or in response to infection by parasitoid wasps[18]. This organ contains prohaemocytes (haematopoietic progenitors) in the medullary zone, kept in a pluripotent stage by the activation of the JAK-STAT pathway[21]. Throughout normal larval development, prohaemocytes migrate towards the cortical zone, where they enter distinct cellular lineages and sequentially express different genetic markers. The specification of plasmatocytes requires the transcription factors Glial cells missing (Gcm) and Gcm2 and crystal cell fate determination is dependent on the cell-autonomous expression of the transcription factor Lozenge (Lz), in a Notch-dependent manner[21,22]. Depending on the maturation stage, plasmatocytes can be identified by the expression of genes such as *hemolectin* and the phagocytosis receptor Eater, and crystal cells by the presence of Lozenge (Lz) or Prophenoloxidase A1 (ProPOA1)[15,22].

In homeostasis, plasmatocytes constitute around 90% of the haemocyte population, while crystal cells account for the remaining 10%[15]. Such levels are maintained throughout the haematopoietic process not only by the LG but by two other compartments. One of them includes the pool of circulating haemocytes that move freely in the haemolymph and take part in the surveillance of the larval body against microbes[15,23]. The other compartment comprises the sessile haemocyte clusters under the dorsal subepidermal layer of the larva, which was recently determined to also be a true hematopoietic tissue[15,20]. This tissue, composed of sessile haemocyte pockets, contributes greatly to the storage, multiplication and differentiation of blood cells, and is likely to be in dynamic equilibrium with the circulating compartment, with which there is constant exchange of cells in both directions[16,24]. Moreover, these sessile clusters are fundamental to the increase of the haemocyte pool and their structure is necessary to achieve a correct proportion between the different types of cells in the larva[20]. However, contrary to what is established to occur in the lymph gland, where crystal cells differentiate from prohaemocytes, in the sessile clusters they transdifferentiate *de novo* from mature plasmatocytes[20]. Both of these compartments consist of groups of plasmatocytes and crystal cells that function as a way of easily mobilizing cells towards, for instance, an effective immune response[15]. After pupariation, haematopoietic tissues disintegrate and only part of the haemocytes created during larval stages remains in the adult[15]. It was recently proposed that a third stage of haematopoiesis occurs during adulthood, guaranteed by four haematopoietic blood cell clusters in the dorsal side of the abdomen. These haemocytes were shown to contribute to phagocytosis of bacteria and blood cell specification[25].

The normal proportions of haemocytes can be disrupted in several circumstances, particularly when lamellocytes differentiate. Sterile wounding and parasitoid wasp eggs laid in *Drosophila* larvae

trigger lamellocyte differentiation in the LG and sessile haemocyte clusters[15,26,27]. In the LG, wasp parasitism induces disruption of JAK-STAT signalling through the action of a *domeless* antagonist, *lat*, in the medullary zone, allowing the differentiation of prohaemocytes[28]. These LG-derived lamellocytes appear at a relatively late stage of the response to parasitoid wasp infection, suggesting that the sessile compartment contributes greatly to the initial increase in lamellocyte numbers. A recent study reported that circulating haemocytes, via the production of the cytokines Upd2 and Upd3, activate JAK/STAT signalling in the somatic muscles and that such process is required for both lamellocyte differentiation and efficient encapsulation of parasitoid wasp eggs[29]. It is further established that lamellocytes transdifferentiate from plasmatocytes, which go through distinct intermediate stages of differentiation and loose phagocytic activity until they reach a terminally differentiated lamellocyte fate[30]. The ectopic differentiation of lamellocytes, as it is also described in some JAK/STAT and Toll pathway mutants, can further lead to the formation of melanotic tumors due to encapsulation of self-tissue[31].

Despite the described role of haemocytes in phagocytosis, wound healing and encapsulation, the contribution of cellular defense mechanisms to the systemic immune response is still unclear. It has been previously reported that, during the larval immune response to orally administered pathogens, plasmatocytes contribute to an efficient activation of AMP production by the fat body cells[32]. In contrast, in adult flies after septic injury blood cells are not required to mount normal Toll and Imd pathway activation[32]. However, plasmatocyte removal has been correlated with increased susceptibility to specific bacterial infection in adult flies[32,33]. Regardless, this vast array of mechanisms culminates in a highly orchestrated immune response against invading organisms in *Drosophila*, where both the humoral and cellular components play important roles in the neutralization and elimination of pathogens, respectively.

1.2 microRNAs: Biogenesis and Function

Since the discovery of *lin-4* and *let-7* in *Caenorhabditis elegans* a large number of microRNAs (miRNAs) have been described in a wide variety of organisms. These discoveries led to the conclusion that this class of noncoding RNA molecules represented a new layer of regulation of gene expression. miRNAs are currently characterized as short non-coding sequences that function through silencing of gene expression, by base-pairing with the 3' untranslated regions (3'UTRs) of target messenger RNAs (mRNAs)[34]. Each one of these sequences targets hundreds of mRNAs, resulting in a broad effect on the mRNA and protein content of cells and making miRNAs one of the main emerging regulators of a wide variety of biological processes[24,35].

miRNAs are produced according to a multi-step process occurring both inside the nucleus and the cytoplasm of cells[34] (Figure 1.2). These sequences can either be found in (1) regions of the genome that are quite distant from the annotated targets, implying that they constitute a different transcriptional unit, or (2) be included inside intronic regulatory regions, providing a mechanism to maintain a coordinated expression between proteins and their respective miRNAs[36]. Some miRNAs can be found organized in clusters, constituted of groups of sequences which are evolutionarily related to each other and often coexpressed[37].

What is known from most animal models is that the majority of miRNA genes are transcribed by RNA polymerase II (Pol II)[36]. The transcription of a miRNA gene generates a stemloop containing the primary miRNA (pri-miRNA)[38], which is processed within the nucleus by a multiprotein complex called the Microprocessor, of which the core components are the RNase III enzyme Drosha and the double-stranded RNA-binding domain (dsRBD) protein DGCR8/Pasha. This complex cleaves the pri-miRNA stem loop, producing an hairpin precursor miRNA (pre-miRNA) that is around 70 nucleotides long[34]. Next, after translocation to the cytoplasm, the pre-miRNA is cleaved again by Dicer to produce the mature ~22-nucleotide miRNA:miRNA* duplex. Dicer, an RNase III endonuclease, was first

implicated in the production of interference RNAs (RNAi) and then recognized as important for miRNA maturation[36].

Following the cleavage steps, the main RNA silencing pathways (siRNA and miRNA) converge and become biochemically indistinguishable[36]. The Argonaute proteins (Ago) are recruited and, together with Dicer, form a trimeric complex that initiates the assembly of the RNA-induced silencing complex (RISC)[34]. Once a single stranded miRNA is incorporated into RISC, the complex is guided to mRNA targets based on base-pairing interactions. Base-pairing with the 5' end of miRNAs, especially to the so-called 2–7 nucleotide 'seed', is crucial for efficient targeting. In cases of perfect or near-perfect complementarity to the miRNA, target mRNAs are cleaved and degraded; imperfect miRNA-mRNA hybrids lead to translational repression[36]. The repression mechanism is far more common and it is achieved by a destabilization of the mRNA sequence. The post-transcriptional step at which silencing occurs is still unclear, but either elongation of the transcript or initiation of translation are the most likely targets[34].

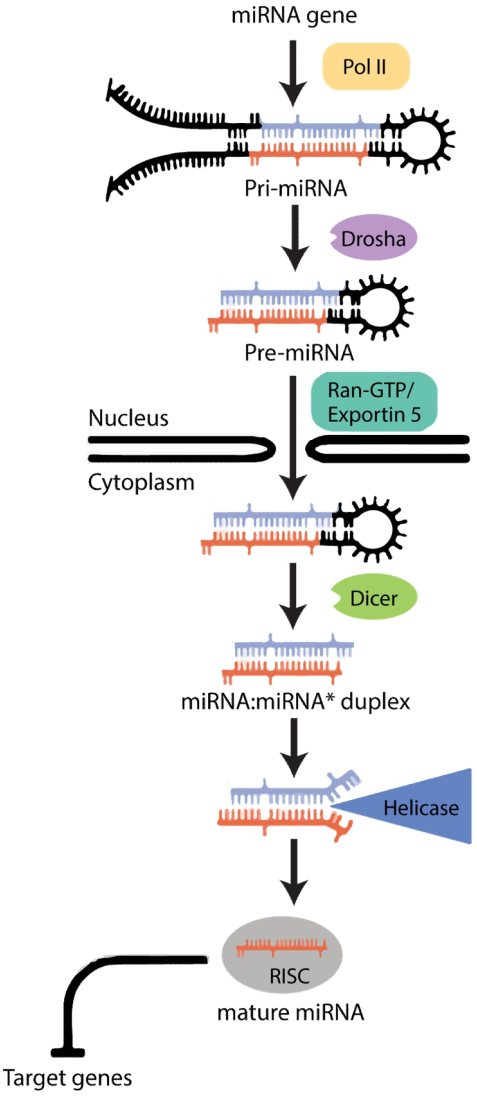

Figure 1.2 – The biogenesis of microRNAs in *Drosophila melanogaster*. After a miRNA is transcribed, the generation of a mature miRNA includes both nuclear and cytoplasmic maturation, culminating in the repression of the translation of several target genes (Adapted from Bartel *et al* (2004)).

Most biological processes are governed by highly regulated activation and suppression of specific gene programs that are dependent on the activity of miRNAs[35]. These sequences are involved in animal development, in cell proliferation and differentiation, in apoptosis and in many other physiological and pathological processes[34]. Furthermore, due to their overlapping functions and "buffering effect" on gene expression variation, they are reported to be crucial for the robustness of developmental and physiological processes[39]. In *Drosophila*, one of the most important miRNAs, *bantam*, was isolated by gain-of-function assays that revealed its capacity to promote tissue growth and inhibit apoptosis[40]. *miR-14* is also involved in this process, as well as in the regulation of fat metabolism in a dose-dependent manner[41].

1.3 microRNAs and the immune response

The regulation of the development and function of the immune system lies among the many processes in which miRNAs have been implicated in vertebrates. This includes the regulation of several components of the vertebrate immune response[24]. Indeed, it is known that miRNAs are differentially regulated in haematopoietic cell lineages, as well as in a vast array of features of host-pathogen interactions[42]. Individual miRNAs have been implicated in Haematopoietic Stem Cells

(HSCs) biology, contributing to their homeostasis and lineage commitment (e.g. mir-196b, mir-221 or mir-222)[43]. miRNAs also have a role in the development and function of vertebrate immune cells, modulating key steps of cellular lineage determination[42]. This includes cells of the mammalian innate immune system, like granulocytes or monocytes from the myeloid lineage (e.g. mir-21, mir-196, mir-181a, mir-223 or mir-150)[43] and the production of Toll-Like Receptors (TLRs) with a major role also in vertebrates in the recognition of invading bacteria, viruses and other pathogens[24]. Furthermore, miRNAs have been reported to be important for the regulation of several adaptive immunity components, such as development of B and T cells, antibody class switching and cytokine production (e.g. mir-17-92 cluster, mir-155 or mir-150) [42]. Importantly, altered expression levels of miRNAs have been implicated in various haematopoietic disorders, such as leukaemias, lymphomas and even cancers with immune cell origin[42].

However, the repertoire of described immune-related miRNAs and their impact on invertebrate immunity is limited and remains largely unexplored. Commonly observed in various host–pathogen systems is a differential abundance of host miRNAs following an infection, which varies over time and according to the type of pathogen involved[44]. Several miRNAs have been implicated in the anti-viral immune response. In this case, abundance of several host miRNAs can be altered after infection in *Bombyx mori* or *Aedes* mosquitoes, where it has been speculated that these sequences could target viral genes, dampening replication rates[44]. This modulatory effect of pathogens on the host miRNA profile is also reported during bacterial infection. This includes, for instance, the effect of *Wolbachia* infection in the miRNA profile of *Aedes aegypti*, where aae-miR-2940 and -309a are reported to have an increase in expression after infection. Also, infection by the Gram-negative bacterium *Serratia marcescens* in *Apis mellifera* leads to the downregulation of miRNAs such as ame-bantam, -mir-12, -34, -184, -278, -375, -989 and -1175, and the upregulation of let-7, ame-mir-2, -13a, and -92a[44]. The available information has been so far obtained from microarray experiments and therefore still lacks vital functional analysis and validation. One of the very few miRNAs whose role in insect immunity has been experimentally established is mir-8, which negatively regulates AMPs such as Drosomycin and Diptericin in *D. melanogaster*[45]. The miRNA let-7 has also been hypothesized to regulate *Diptericin* expression in *Drosophila* S2 cells through the action of the hormone Ecdysone. By repressing Diptericin translation in an ecdysone-dependent manner, let-7 may set a threshold for this AMP and possibly avoid over-stimulation of the innate immune response[46]. But the complete function of these sequences in the immune system of invertebrates has yet to be fully understood. Taking into account that immune mechanisms are relatively well conserved among animals, further characterization of miRNA-mediated gene regulation during haematopoiesis should shed light on the homeostatic control of haematopoietic cell renewal and differentiation, while characterization of the humoral response should provide insights on several important features of host-pathogen interactions.

In order to dissect the role of miRNAs in the regulation of immune-related mechanisms in *Drosophila melanogaster*, we propose to address two main questions that focus on each of the arms of the immune system: the humoral and the cellular defences. It is known that the success of haemocyte function depends on their numbers and proportions. Hence, any defects in haematopoiesis, the developmental process that regulates haemocyte proliferation and differentiation, will compromise the availability of these cells throughout development. Our questions include (1) understanding the impact of miRNAs in the control of larval haematopoiesis, the most active and well characterized stage of this developmental process, and (2) dissecting the role of miRNAs in the regulation of the humoral response, mainly involved on the recognition of invading organisms and the triggering of the systemic antimicrobial response.

2. Materials and Methods

2.1 Fly Stocks and Maintenance

To identify miRNAs that modulate larval haematopoiesis and the adult systemic immune response we performed a systematic screen using a library of knock-out lines generated by ends-out homologous recombination by Cohen *et al*, 2014, covering the vast majority of the miRNAs present in the genome of *D. melanogaster*. This library encompasses 75 loci encoding a set of 130 single miRNA precursors, and 20 miRNA clusters encoding a total of 58 different miRNA precursors[47]. Both single and multiple knock-out of abundant and evolutionarily conserved sequences were used, in which each deletion inactivates single miRNAs or the 8-nucleotide seed of a given cluster of miRNAs respectively. Due to availability constraints, our study focused on a panel of 83 out of the 95 lines of the original library (Supplementary Data – Table 1).

This panel of *Drosophila melanogaster* microRNA knock-out lines was kindly provided by Claudio Alonso Lab, University of Sussex, UK (Supplementary Data - Table1). The controls y^1,w^* and w^{1118} together with all microRNA deletion lines were simultaneously crossed with the balancer chromosomes y^1, w^*, $N^1/FM7c$, *P{w[+mC]=GAL4-twi.G}108.4*, *P{UAS-2xEGFP}AX*, w^{1118}; *In(2LR)Gla*, $wg^{Gla\text{-}1}$/ *CyO*, *P{w[+mC]=GAL4-twi.G}2.2*, *P{UAS-2xEGFP}AH2.2* and w^*; $ry^{506}Dr^1$/ *TM3*, *P{Dfd-GMR-nvYFP}3*, Sb^1. Due to higher genetic background disparities, lines including miRNAs located on the chromosome X were crossed with the control y^1,w^* for an extra generation (Supplementary Data – Figure1). Due to differences in lethality between the different microRNA deletion lines (Supplementary Data – Table1), the screening process was performed in two modalities: (1) homozygous lethal mutations were tested in heterozygosity over a balancer or over a wild type chromosome; (2) the remaining lines were tested as homozygous. Depending on the modality, lines were compared to equally balanced or non-balanced controls. All fly stocks were maintained in standard fly food at 18ºC. Crosses and experiments were performed at 25°C, ~60% humidity and 12:12hr light:dark cycles.

2.2 Systemic Immunity Screen and Bacterial Infection

Pseudomonas entomophila and *Pseudomonas putida* were used for systemic infection in the primary and secondary systemic immunity screens respectively. Following Martins *et al* (2014), bacterial stocks were kept in glycerol at -80 ºC, streaked in fresh Petri dishes and incubated at 30 ºC. Before use single colonies were picked and let to grow overnight at 30 ºC in Lysogeny Broth medium (LB). Cultures were centrifuged and adjusted to the desired optical density (OD, 1=5x10^8cells/mL) (*P. entomophila*, OD~0,01; *P. putida*, OD~10). For each of the lines tested and their respective controls, adult flies (4–6 days after eclosion) were pricked in the thoracic region with a tungsten needle soaked in bacterial solution. Sterile LB medium was used for technical controls on control lines (X, 2 and 3). Each of the biological replicates included administration of bacterial treatments to 30 to 50 males, after which individuals were separated in random groups of 10 on small tubes with standard fly food and kept at 25ºC, ~60% humidity and 12:12hr light-darkness cycle. Survival was monitored every day for 6 days in the case of *P. entomophila* and 7 days for *P. putida*. Individuals that did not recover from anaesthesia after 2h or were alive at the end of the experiment were counted as censored observations.

2.3 Haematopoiesis Screen, Larval Imaging and Cell Counting

Crystal cells and plasmatocytes were labelled with specific live genetic fluorescent markers on all mutant lines to perform the haematopoiesis screen and analyze several features of differentiation

and proliferation of larval haemocytes. Depending on the location of the microRNA deletion, the markers were distributed across the genome in three different combinations: *w*; eater-DsRed; BcGFP*, or *LzGal4, EaterGFP; +/+; UAS-Tomato* or *LzGal4, UAS-mCD8GFP; eater-DsRed; +/+*. Note that Eater marks plasmatocytes whereas Lozenge (Lz) and Black Cells (Bc) are crystal cell markers. The genetic crosses required to create lines carrying the cell reporters as well as each of the microRNA knock-outs were also carried out on the existing controls for each of the chromosomes analyzed. The sessile haemocyte compartment, particularly on the most posterior segment of the larval body, was used as a proxy for the remaining segments as previously validated[48]. All experiments were performed in males, due to high variance associated to the haemocyte pool of females.

Ten late third instar (L3) male larvae were imaged for each of the screened lines. After staging and male selection, larvae were placed in a microcentrifuge tube with standard fly food at room temperature (RT) for at least one hour before imaging. Prior to acquisition, the selected larvae were washed twice in cold 1xPBS, dried on paper and placed on a cold metal block. Individual larvae were secured under a microscope slide and imaged dorsally on a Zeiss STereo LUMAR stereoscope equipped with a Hamamatsu Orca-ER CCD camera and a GFP fluorescence filterset. Together with a whole-body picture, a high-magnification caption was taken of the posterior-most haemocyte cluster of the larval body for quantification purposes. Cells were counted on Fiji[49] to assess proportions and density. Plasmatocyte numbers and cluster area were determined automatically using the ITCN plugin[50] and crystal cells were counted manually using the Cell Counter plugin[51].

2.4 Lymph Gland Dissection and Haemolymph Extraction

Detailed description of the phenotype of the miR-980 knock-out line required further crossing with: (1) *+/+; eaterGal4, UAS-YFP, MSNF9-mCherry; BcCFP* for labelling lamellocytes (MSNF9-mCherry) and the remaining types of haemocytes; (2) w^{1118}*; 10XStat92E-GFP* for reporting activation of the JAK-STAT pathway. For lymph gland characterization, late L3 male larvae resulting from these crosses were collected and dissected according to Evans *et al* (2014). Samples were fixed for 30 minutes in 3.7% ρ-formaldehyde:PBS at RT, washed three times with 1xPBS for 5 minutes and mounted on a microscope slide with Vectashield (Vector). Confocal Z-series stacks were acquired on a Leica SP5 confocal using 20x and 40x air objectives. The circulating haemocyte compartment was characterized according to Leitão&Sucena (2015). Six L3 male larvae were disrupted on the ventral cuticle to minimize inclusion of cells from the dorsal clusters. Haemolymph from the dissected larvae was collected and placed on a 12-well slide for 20 minutes. Following fixation with 3.7% ρ-formaldehyde:PBS for 20 minutes, samples were washed three times with 1xPBS and sealed in Vectashield. Images were acquired on a Leica DMRA2 upright microscope using the 20x air objective.

2.5 Statistical Analysis

Statistical analysis and graphics were done on R Studio, version 3.2.2, and GraphPad Prism Software, version 6. Survival fractions for each time point were estimated using the Kaplan-Meyer method and analyzed in two statistical approaches: (1) Comparison of average survival curves using the Logrank (Mantel-Cox) test; (2) Comparison of hazard ratio regression coefficients using a Cox's proportional hazards mixed effect model. The first approach allows comparison of survival curve dynamics over time, taking into consideration each time point. The Logrank comparison in particular gives equal weight to all time points. The second approach provides a global estimate of the risk of death after infection (hazard ratio), while allowing the exploration of the effects of several explanatory variables on survival. Due to the detection of a significant difference between biological replicates (date effect), hazard ratios were analyzed with the mutant lines defined as a fixed factor and date of the experiment and replicate vials were defined as random factors. Hazard ratios of independent trials for

each mutant line were also taken in consideration. Data obtained from the haematopoiesis survey was checked for normal distribution using a Saphiro-Wilk test. Samples were compared with their controls using t-tests when normally distributed and a Wilcoxon–Mann–Whitney test when the distribution departed from normal. Multiple comparisons from both datasets were corrected using the Bonferroni or the Holm-Bonferroni tests.

2.6 Retrieval of computationally predicted miRNA targets

microRNA predicted target retrieval was done using an online database based on several algorithms designed for this purpose (http://m3rna.cnb.csic.es/)[52]. These algorithms consider properties like complementarity and structure of the miRNA-mRNA interaction and attribute each target gene different scores based on such features. There are two combinatorial approaches of several available predictive algorithms in order to make predictions more efficient: (1) Weighted Scoring by Precision (WSP), based on summing up the weighted scores for different databases and (2) Logistic Regression combined Scoring (LRS), which applies logistic regression to find the combined score of the algorithms taking in consideration the probability of experimental validation[52]. LRS was preferentially used to assess the high score targets for each of the obtained candidate microRNAs and only the first 200 high-LRS score target genes for each miRNA were considered.

3. Results

3.1 microRNAs have a role in systemic immunity of *Drosophila melanogaster*

To assess if microRNAs play a role in the systemic immune response of *Drosophila*, we performed a primary screen on eighty-three different microRNA (miR) deletion lines by monitoring survival of adult flies after infection with *Pseudomonas entomophila*.

In general, results from the statistical comparisons of both survival curves and hazard ratios between controls and treatments are in agreement with each other (Supplementary Data – Table 2). However, some miRNA deletions report significant differences in the hazard ratios without producing detectable differences in the comparison of survival curves or *vice-versa*. Furthermore, analysis of the hazard ratios of independent biological replicates revealed that detectable differences are not always consistent among trials (Figure 3.1). Based on these distinct statistical outcomes the lines tested were stratified into four categories:

Rank 1 includes 14 lines which show consistent differences in both statistical approaches when compared to their controls (Supplementary Data – Table 2). Hence, mutations included in this category significantly impact the risk of death after infection, generating very distinct survival dynamics over time. For instance, mir-990 deletion causes a striking decrease in survival after the first day of infection that is corroborated by a high hazard ratio coefficient, consistent across all biological replicates. Other lines, such as mir-137 and mir-285 deletions, report the same outcome, but independent replicates reveal disparate tendencies (Figure 3.1). s

Rank 2 represents situations where significant differences in the survival curves between treatment and controls were reported, but hazard ratio comparison failed to corroborate these findings. For example, the accentuated increase in survival after infection of mir-100/let-7/mir-125 deletion line that is detected in the survival curve comparison, fails to be represented by a significant negative hazard ratio (Figure 3.1 – D), which is only mildly detected in one of the biological replicates.

Rank 3 refers to situations where hazard ratios were significantly different between treatments and controls, but overall survival curves were not distinct enough to validate their disparity.

Rank 4 includes the remaining lines, where all statistical tests were negative.

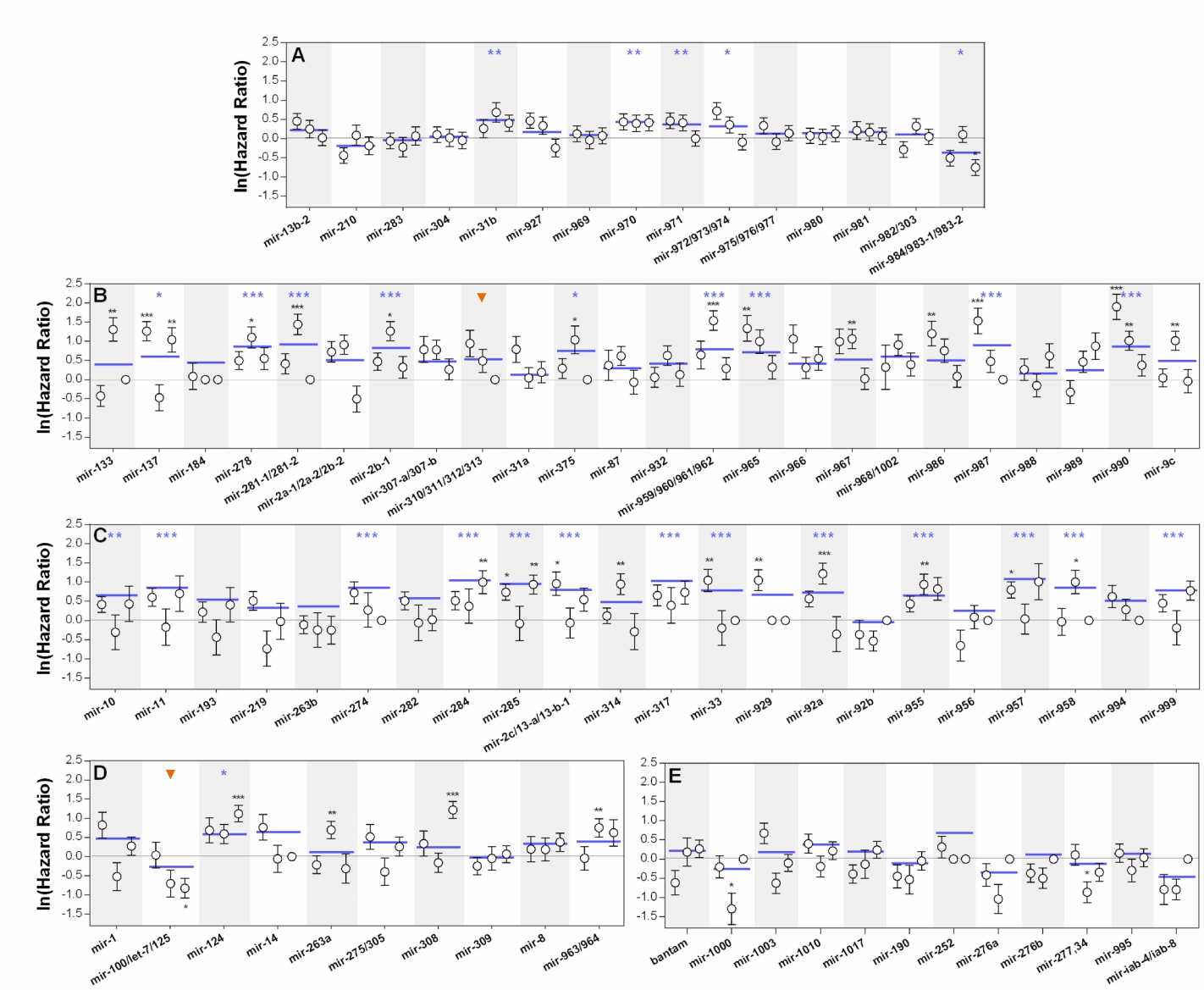

Figure 3.1 – Survival to bacterial infection. Natural logarithm of hazard ratios between survival of flies with knocked-out microRNA genes and their controls upon infection with *P. entomophila*. (**A**) microRNA knock-out lines located on the X chromosome. (**B**) Homozygous viable microRNA knock-out lines located on chromosome II and (**C**) III. (**D**) Homozygous lethal microRNA knock-out lines located on the chromosome II and (**E**) III. Significant deviations from the control line (x=0) represent significantly different hazard ratios (p<0,05). Positive and negative coefficients represent decreased and increased survival, respectively. White circles represent independent biological replicates of each line and blue lines refer to the hazard ratio obtained from the statistical model that accounts for a random date effect (See materials and methods). Vertical bars correspond to the 95% confidence intervals of the estimated hazard ratios. Data points that overlap with the basal line and lack vertical bars represent missing data. The orange arrowheads represent the two lines belonging to Rank 2, which reported significant differences exclusively for the average survival curve comparisons. *p<0,05; **p<0,01 ; ***p<0,001.

This ranking system was used to select the lines used in the subsequent phases of the screening process. We performed our secondary screen on fifteen candidates, including lines to which Rank 1 was attributed based on three biological replicates (13 lines) and two extra lines from Rank 2 that showed interesting differences in the overall survival curves dynamics. This screen consisted of a *Pseudomonas putida* systemic infection. Figure 3.2 represents the normalized hazard ratios obtained for the candidate microRNA deletion lines upon infection with *P. putida*. Out of the 15 lines considered, only five reported significant differences in survival after infection (p<0,05). The same differences were consistent between the comparison of survival curves and of hazard ratios (Supplementary Data – Table 3 and Figure 3). These include mir-31b, mir-2b-1 and the mir-100/let-7/mir-125 cluster, which show a significant increase in survival when compared to controls, and mir-137 and mir-317 that had a significant decrease in survival after bacterial infection. Importantly, due to time constraints this dataset refers to only one trial. Further replication is necessary to firmly establish a role for these candidate microRNAs in the immunity of *Drosophila melanogaster* against *Pseudomonas* systemic infection.

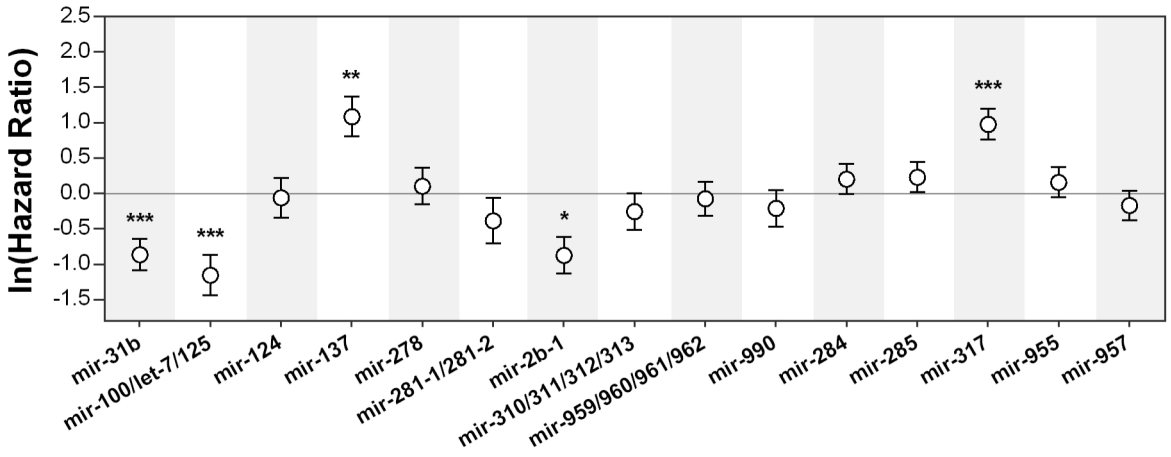

Figure 3.2 – Survival to bacterial infection of candidate microRNA knock-out lines. Natural logarithm of hazard ratios between survival of flies with knocked-out microRNA genes and their controls upon infection with *Pseudomonas putida*. The basal line refers to the controls of each sample, thus significant deviations from zero represent significant differences in survival (p<0,05). Positive and negative hazard ratio coefficients represent decreased and increased survival, respectively. Vertical bars correspond to the 95% confidence intervals of the estimated hazard ratios. *p<0,05; **p<0,01; ***p<0,001.

Throughout our trials, the observed phenotype of candidate microRNA deletions was found to be relatively consistent in some lines, while others showed reverse tendencies. This is the case of the mir-31b and mir-2b-1 deletions, which reported opposite survival tendencies between screens performed with different pathogenic bacteria from the genus *Pseudomonas*. The remaining lines that revealed significant differences were consistently susceptible or resistant/tolerant to bacterial infection – mir-100/let-7/mir-125 cluster, mir-137 and mir-317. Based on our observations, we then asked which genes could be targeted for post-transcriptional silencing by these miRNAs. Among the extensive list of target genes found to be complementary to our candidate miRNAs, we found annotated ontology categories associated with regulation of the general antimicrobial immune response, particularly of the Imd, Toll, JNK and JAK-STAT pathways (Table 3.1). Furthermore, some of the lists included genes that have annotated roles in both systemic and cellular immunity, particularly in haematopoiesis (Supplementary Data – Table 4).

Table 3.1 – Retrieved immune-related target genes for candidate miRNAs obtained from the systemic immunity screens

miRNA	Target Gene	LRS score	Annotated Function
mir-31b	*zfh1*	0.972939	Antimicrobial humoral response
	mask	0.335379	Antimicrobial humoral response
	puc	0.178504	JNK cascade Positive regulation of the immune response
mir-100	*Socs36E*	0.183429	Negative regulation of JAK-STAT cascade
	Crk	0.0602045	Positive regulation of JNK cascade
	Su(var)2-10	0.0265506	Defense response to Gram-negative bacterium Positive regulation of innate immune response
	heix	5.23E-05	Regulation of Toll signalling pathway
	GATAe	4.49E-05	Antimicrobial humoral response
	dome	4.09E-05	Defense response to Gram-negative bacterium Negative regulation of innate immune response JAK-STAT cascade
	slpr	2.62E-05	JNK cascade
	park	2.18E-05	Negative regulation of JNK cascade
let-7	*hep*	0.396529	Melanization defense response Positive regulation of JNK cascade
	lola	0.395459	Antimicrobial humoral response
	A3-3	0.384036	Immune response
	IM2	0.23867	Defense response
	CBP	0.060222	Defense response to Gram-negative bacterium
	hop	0.0265521	Defense response to virus Regulation of JAK-STAT cascade
	spen	0.0265516	Defense response to fungus
mir-125	*lola*	0.989636	Antimicrobial humoral response
	PGRP-LD	0.178505	Immune response
	Stat92E	0.0601793	Humoral immune response Regulation of JAK-STAT cascade Defense response
	Rala	0.026548	Innate immune response Defense response to Gram-negative bacterium Negative regulation of innate immune response
	CG13890	0.026548	Defense response to Gram-negative bacterium
	Rab6	0.000141138	Defense response to fungus
	nimB2	3.48E-05	Defense response to bacterium
mir-137	*dup*	0.978351	Antimicrobial humoral response
	CG12004	0.978236	Defense response to fungus
	par-1	0.978236	Antimicrobial humoral response
	CG14411	0.395535	Defense response to Gram-negative bacterium
	kay	0.395476	Antimicrobial humoral response
	PGRP-LB	0.395458	Defense response to Gram-positive bacterium Negative regulation of PGRP signalling pathway
	scrib	0.978927	Positive regulation of Amp production
mir-317	*Pli*	0.383579	Toll signalling pathway Negative regulation of Toll signalling pathway
	Rab6	0.337308	Defense response to fungus
	CG5899	0.183368	Defense response to Gram-negative bacterium
mir-2b	*psh*	0.9874480	Defense response to fungus Innate immune response
	Tab2	0.4450730	Response to bacterium PGRP signalling pathway Positive regulation of defense response to virus
	upd1	0.3837370	Defense response to Gram-negative bacterium Negative regulation of innate immune response
	BobA	0.3359690	Defense response to bacterium
	18w	0.2386640	Immune response Antibacterial humoral response

3.2 The role of microRNAs in the haematopoiesis of *Drosophila melanogaster*

The combined action of both humoral and cellular arms during the immune response of *D. melanogaster*, together with the indication that miRNAs can have several haematopoiesis related targets, led us to ask if miRNAs could play a role in haematopoiesis and cellular immunity. To tackle this, we performed a screen on the same panel of microRNA knock-out lines used above for haematopoietic defects. Using the most posterior sessile haemocyte cluster of the larval body as a proxy for total sessile haemocytes[48], we quantified the following haematopoietic features of larvae: plasmatocyte and crystal cell absolute numbers and sessile cluster size. These two measurements were used to determine the densities of each cell type in the sessile haematopoietic compartment (cells/μm^2). Figure 3.3 refers to larval haemocyte densities at the posterior-most cluster of the several microRNA deletion lines analyzed. Due to time constraints and crossing scheme limitations, only deletions located on the X chromosome (Figure 3.3 – A) and homozygous lethal from second and third chromosomes were included in our analysis (Figure 3.3 – B and C).

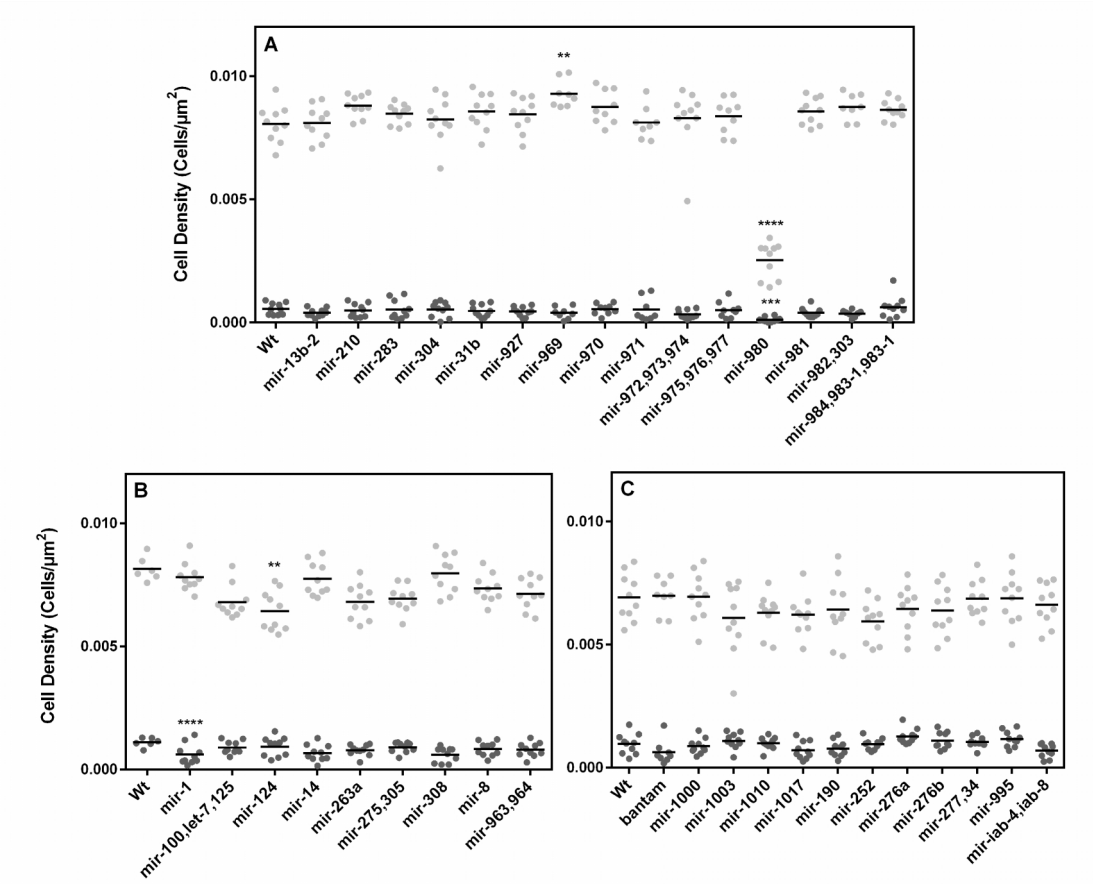

Figure 3.3 – **Plasmatocyte and crystal cell density.** Quantification of plasmatocyte (●) and crystal cell (●) densities in the most posterior sessile haemocyte cluster of L3 male larvae (Number of cells/Cluster Area, Cells/μm^2). Black horizontal lines refer to the mean of each dataset. (**A**) Plasmatocyte and crystal cell density of microRNA knock-out lines located in the X chromosome and of homozygous lethal microRNA knock-out lines located in the (**B**) chromosome II and (**C**) III. *p<0,05; **p<0,01 ; ***p<0,001; ****p<0,0001.

Out of a total of 36 lines analyzed for this trait, four showed significant changes in either plasmatocyte and/or crystal cell densities (p<0,05): mir-969, mir-980, mir-1 and mir-124.

mir-969 hemizygous deletion shows a small yet significant increase in plasmatocyte density (Figure 3.3 – A) as a result of having reduced clusters that maintain average plasmatocyte numbers (Supplementary Data – Figure 4 and 5).

mir-980 hemizygous knock-out produced a striking decrease in the densities of both cell types (Figure 3.3 – A). Despite being associated with a reduction in cluster size (Supplementary Data – Figure 4), this is not significant, indicating that the detected differences in density are in fact a result of a marked decrease in cell numbers (Supplementary Data – Figure 5 and 6).

Additionally, mir-1 heterozygote knock-out shows a considerable decline in crystal cell density (Figure 3.3 – B) likely due to the observed non-significant decrease in crystal cell numbers (Supplementary Data – Figure 6).

Finally, mir-124 heterozygous deletion is associated with a reduction in plasmatocyte density (Figure 3.3 – B), again associated with a non-statistically detectable reduction in plasmatocyte numbers (Supplementary Data – Figure 5).

Collectively, our observations point towards the idea that microRNAs are important regulators of haematopoiesis. Among the predicted target genes of each of the miRNA candidates obtained from this screen, and reinforcing our observations, we found genes with annotated roles in haematopoiesis, JAK-STAT and Notch signalling and crystal cell differentiation, as well as cell adhesion and extracellular matrix assembly (Table 3.2). Further characterization of the remaining lines of the microRNA knock-out panel could reveal other important players in the dynamics of proliferation and differentiation in haematopoiesis that ultimately can influence other developmental processes and biological responses.

Table 3.2 – Retrieved immune-related target genes for candidate miRNAs obtained from the haematopoiesis screen.

miRNA	Target Gene	LRS score	Annotated Function
mir-980	*tub*	0.9813450	Haematopoiesis
	RanBPM	0.9813450	JAK-STAT cascade
	dome	0.1837420	JAK-STAT cascade
mir-1	*mam*	0.9952790	Notch signalling
	VhaAC39	0.4441350	Regulation of Notch signalling
	Dap160	0.4440740	Negative regulation of Notch signalling
	Nedd4	0.3957160	Negative regulation of Notch signalling
	Su(H)	0.3955080	Crystal cell differentiation Notch signalling
	aux	0.3840240	Notch signalling
	E(bx)	0.3362240	Haematopoiesis
mir-969	*vav*	0.2122100	Cell adhesion Regulation of adherens junction organization Actin cytoskeleton reorganization
	gho	0.1785050	Positive regulation of cell-cell adhesion
	Abi	0.1785050	Cell adhesion Actin cytoskeleton organization Cell adhesion mediated by integrin
mir-124	*wun*	0.9799630	Septate junction assembly Cell migration and repulsion
	tlk	0.9799630	Cell adhesion
	CAP	0.4449310	Cell adhesion
	wts	0.4446600	Negative regulation of cell proliferation
	how	0.3956470	Cell adhesion Mesoderm development
	LanB2	0.3955950	Cell adhesion mediated by integrin Extracellular matrix assembly
	Mmp1	0.3844370	Basement membrane disassembly Extracellular matrix organization Cell-cell junction organization
	Fit1	0.3842700	Cell-matrix adhesion
	Ilk	0.3362870	Cell-matrix adhesion
	Egfr	0.3362190	Regulation of haemocyte differentiation Positive regulation of cell proliferation
	mys	0.3357010	Cell-substrate adhesion Haemocyte migration Cell adhesion mediated by integrin Substrate adhesion-dependent cell spreading

Table 3.2 (continued)			
miRNA	**Target Gene**	**LRS score**	**Annotated Function**
mir-124	*parvin*	0.2386660	Cell adhesion
	girdin	0.2123550	Epithelial cell-cell adhesion
	scb	0.2122480	Cell-cell adhesion Calcium-dependent cell-matrix adhesion
	mbt	0.2122350	Regulation of cell-cell adhesion mediated by cadherin

3.3 mir-980 controls lamellocyte differentiation in the sessile haemocyte clusters

The deletion of mir-980 produced the most striking phenotype obtained from the primary screen for haematopoiesis defects. As shown in Figure 3.4, both crystal cells and plasmatocytes show a marked decrease in density in the sessile haemocyte clusters of mir-980 hemizygous male larvae. This outcome is not correlated with changes in cluster area, but rather with a strong decrease in the absolute numbers of both cell types (Supplementary Data – Figure 4 to 6). Additionally, preliminary observations of lymph gland structure did not reveal similar cellular features, pointing to the idea that such changes could be exclusive of the sessile haemocyte compartment. Additionally, we detected the presence of melanized nodules in the haemocoel of late L3 larvae and pupae. However, such structures were not common to all individuals, being found in around 10% of the population. Furthermore, no fluorescence was detected in dissected nodules for both crystal cell and plasmatocyte specific markers (data not shown).

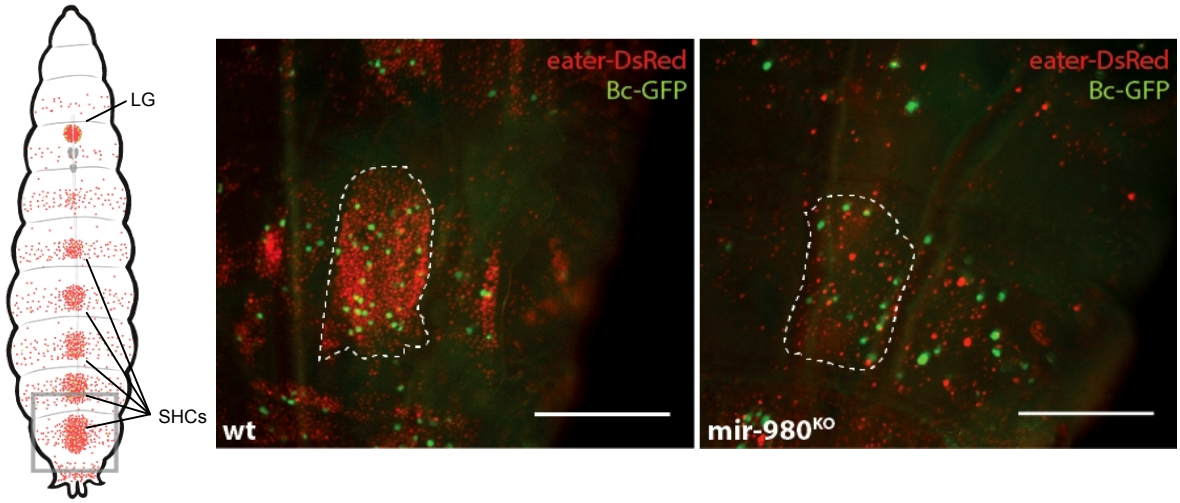

Figure 3.4 – mir-980 knock-out decreases plasmatocyte and crystal cell densities. (Left) Schematic dorsal view of a third instar larva where plasmatocytes and crystal cells are marked in red (eater-DsRed) and green (Bc-GFP), respectively. Highlighted is the most posterior cluster, used as a proxy to infer haemocyte densities (LG, Lymph Gland; SHCs, Sessile Haemocyte Clusters). (Center and Right) Magnified dorsal view of the most posterior haemocyte cluster of mir-980 larvae and the respective control. (scale=250µm)

The presence of melanized nodules in the larval haemocoel is common in previously described mutant phenotypes and is associated in some circumstances with ectopic lamellocyte differentiation[53]. Furthermore, both lamellocytes and crystal cells transdifferentiate from plasmatocytes and depend on the number of the latter cell type[15,20]. We therefore asked if the accentuated decrease in plasmatocyte numbers was caused by a change of cellular fate into lamellocytes. As shown in Figure 3.5 using the lamellocyte specific reporter for the gene *misshapen* MSNF9-DsRed, mir-980 deletion triggers ectopic lamellocyte differentiation and these cells are found circulating in the haemolymph in high numbers. Combined with a reduction in the numbers of plasmatocytes and crystal cells, we confirmed the severe disruption of the integrity of the sessile haemocyte compartment (Figure 3.5 – E and G) and the presence of melanotic nodules in the context of a mir-980 deletion. Furthermore, lamellocyte differentiation was found to occur in the lymph glands (Figure 3.5 – F). However, the fact that this

organ is still intact in the mutant background, contrary to what was expected, suggests that the main contribution to the circulating lamellocyte population comes from the sessile haemocyte compartment only. Staged analysis of the phenotype also revealed that this exacerbated differentiation event begins after larvae reach the mid L3 stage and persists after pupariation, being found also in adults (data not shown). Collectively, our observations suggest that mir-980 plays an important role in inhibiting lamellocyte differentiation in homeostasis.

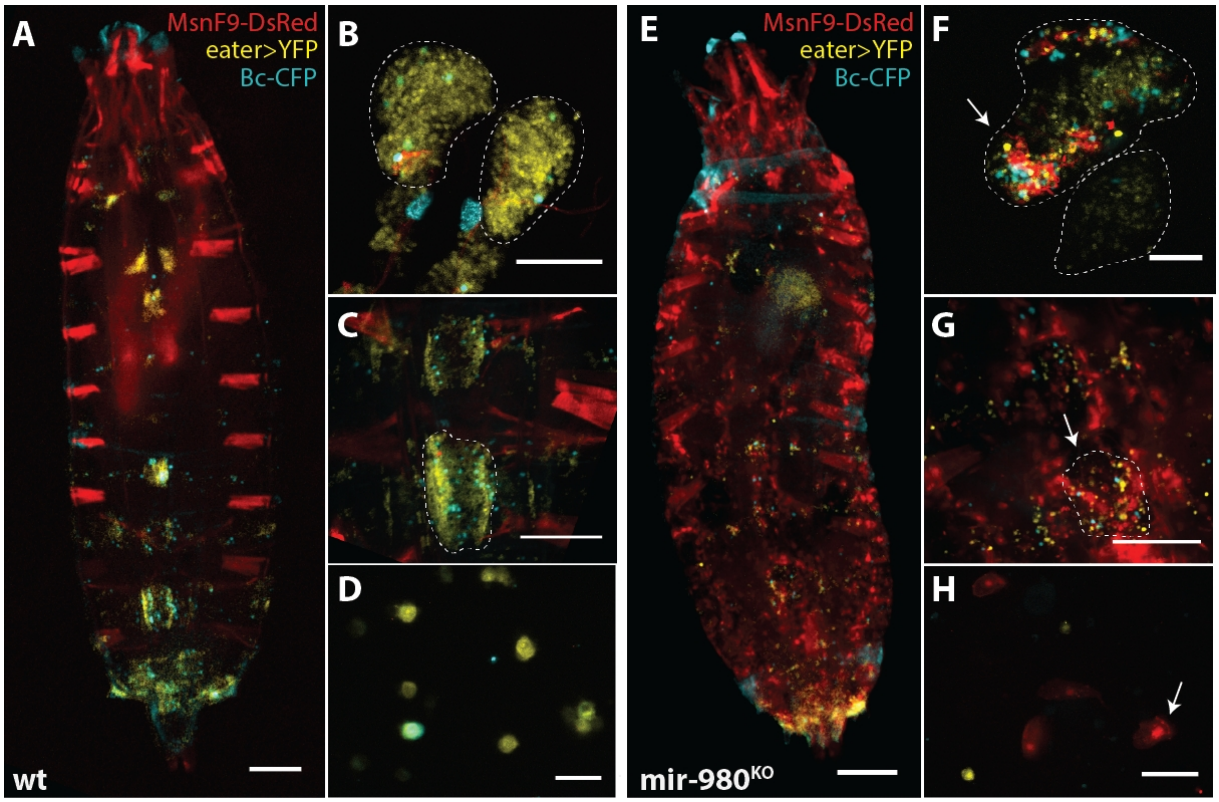

Figure 3.5 – mir-980 has a role in the regulation of lamellocyte differentiation. Comparison of the different haemocyte compartments of third instar male larvae of control line (**A-D**) and mir-980 knock-out (**E-H**). Plasmatocytes are marked with eater>YFP, crystal cells with Bc-CFP and lamellocytes with MsnF9-DsRed. (**A, E**) Dorsal view of the larval body (scale=250μm) together with (**B, F**) dissected lymph glands (scale=100μm), (**C, G**) magnified sessile haemocyte clusters (scale=250μm) and (**D, H**) circulating haemocytes (scale=50μm).

We next asked which gene products could be targeted for silencing by mir-980, ultimately contributing to the regulation of lamellocyte transdifferentiation. Among the high LRS score targets, we found that mir-980 has predicted complementarity to *domeless*, the transmembrane receptor of the JAK-STAT pathway[28] (Table 3.2). Activation of the JAK-STAT pathway has been previously reported to be associated with ectopic lamellocyte differentiation and melanotic nodule formation[11]. Based on the idea that deletion of mir-980 would lead to an increase in dome translation, we assessed the JAK-STAT activation status. Preliminary results show that mir-980 deletion causes a change in the activation pattern of Stat92E (Figure 3.6), the nuclear effector of the JAK-STAT pathway[11]. This is particularly evident in the whole-body expression pattern (Figure 3.6 – D). Whether the change in expression occurs in the epidermis, fat body or any other widespread tissue still remains to be determined. Furthermore, the haematopoietic compartments failed to report strong changes in GFP expression. However, a markedly reduced number of haemocytes shows cytoplasmic GFP expression in the mutant context, both in the lymph glands and in the circulating haemocyte compartments (Figure 3.6).

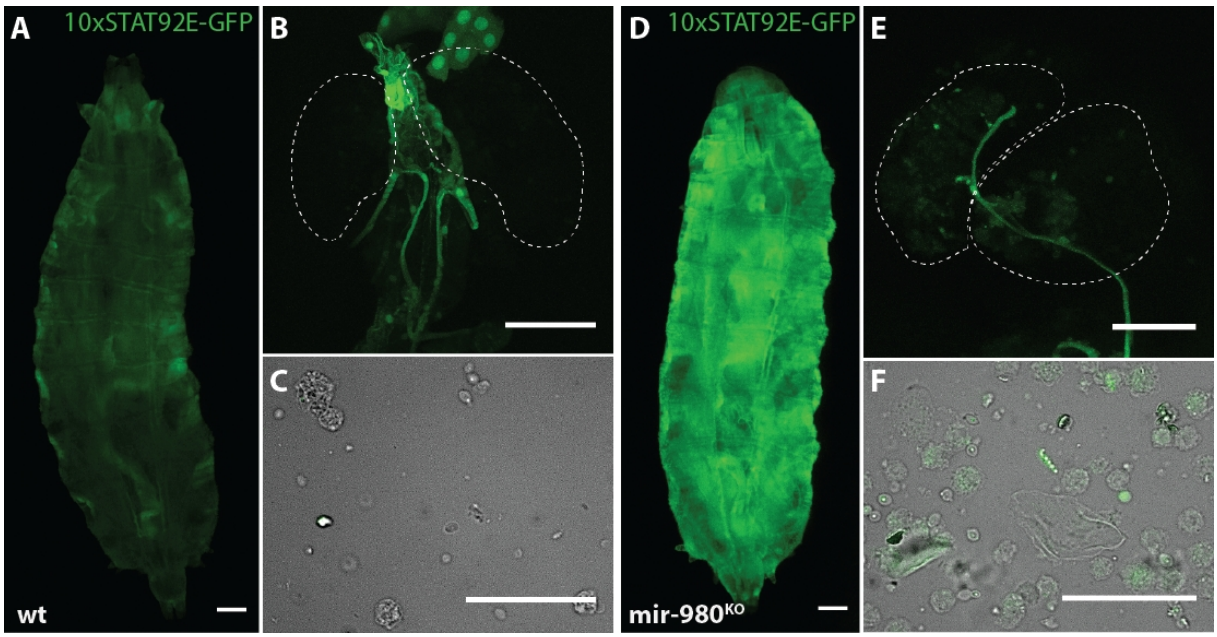

Figure 3.6 – mir-980 knock-out impacts STAT92E expression pattern. Comparison of the STAT92E activation pattern in third instar male larvae of control line (**A-C**) and mir-980 knock-out (**D-F**). (**A, D**) Dorsal view of the larval body (scale=250µm) together with (**B, E**) dissected lymph glands (scale=100µm) and (**C, F**) circulating haemocytes (scale=50µm).

4. Discussion

In this project, we set out to unravel the roles of miRNAs in the immune response of *D. melanogaster* assessing if (1) miRNAs play a role in the humoral defences, particularly in the regulation of susceptibility to bacterial infection and (2) if miRNAs are important for the regulation of cellular defences, mainly in regards with the development of haemocytes.

4.1 Experimental design

Our results from a primary screen of miRNA knock-out lines challenged with *P. entomophila* systemic infection indicate that several miRNA genes are necessary for the regulation of susceptibility to bacterial infection and for the function of general immune defense mechanisms (Figure 3.1). *P. entomophila* is a gram-negative bacterium that has the ability to trigger both local and systemic immune responses after ingestion or systemic administration[54,55]. Furthermore, systemic infection with *P. entomophila* is correlated with high virulence at low doses when compared to the oral infection route, since the first bypasses the epithelial barrier defences inherent to the latter. Therefore, systemic infection leads to high mortality rates even with bacterial concentrations at the lower edge of detection. Steep mortality curves, where mortality reaches a plateau above 85% in the first three days, have low resolution. Hence, small effect mutations which may lead to higher mortality might go unnoticed and create false negatives. Decreasing the 24-hour sampling interval or using "slow-killing" pathogens in the primary screen might have had a positive effect in this loss of resolution. Nonetheless, we chose *P. entomophila* for our initial approach because, contrary to other bacteria, it is a natural pathogen of *D. melanogaster* and is able to trigger Imd activation after systemic infection[2].

Moreover, due to viability constraints, some miRNAs were tested in heterozygosity, which might contribute to the presence of false negatives among our datasets. mir-8, for instance, has been previously implicated in the regulation of AMP levels in homeostasis[45]. However, due to high pupal lethality, it was only tested in heterozygosity and we failed to detect differences in adult survival after bacterial infection (Figure 3.1). Importantly, the detection of a statistically significant date effect

between biological replicates indicates that some differences are influenced by an external variable rather than the infection itself. Thus, survival analysis requires accounting for such explanatory variables (Cox's proportional hazards mixed effect model), rather than just comparing average survival distributions (e.g. Logrank (Mantel-Cox) test). Furthermore, analysing independent biological replicates can hint at whether we are facing generalized and robust survival tendencies or not (Figure 3.1). The lack of sensitivity inherent to the statistical tests has to be taken into consideration also, since even multiple comparison corrections can increase the presence of false negatives within large datasets. Due to such features of the experimental design, our primary set of candidates obtained from infection with *P. entomophila* may underrepresent the extent to which miRNAs regulate the humoral immune defences in *D. melanogaster*.

Notwithstanding, the presence of false positives would have a more prominent impact, particularly in the number of candidates that reach subsequent phases of screening processes. This highlights the importance of validation experiments of the results of high throughput screens, namely assessing carefully data reproducibility either after infection with the same pathogen or a similar one. Thus, we performed a preliminary secondary screen with *P. putida*, a congeneric gram-negative bacterium to *P. entomophila*. *P. putida* is a "slow killer", generally causing slower mortality rates and requiring higher concentrations to achieve the same mortality plateau seen for *P. entomophila*. Our results indicate that, out of a total of 15 lines initially tested from the primary screen, only five report significant differences in the secondary screen: mir-31b, mir-100/let-7/mir-125 cluster, mir-137, mir-2b-1 and mir-317 (Figure 3.2). Such reduction in the number of candidates can be due either to the presence of false positives among our initial list or to the cross-resistance properties between the two bacteria species used. Cross-resistance properties refer to the pathogen-related specificity of the immune response, where different pathogens report divergent lethality and induce distinct responses, even when belonging to the same genus[55]. Due to this aspect, a secondary screen using *P. putida* may fail to validate responses that are specific to *P. entomophila* and any candidate confirmed to fall within this category should be further analyzed in the future. Importantly, this secondary screen would be more robust if represented by three or more replicates, but time constrains allowed us to perform only one. Robust biological replication could imply changes in the validation outcome, contributing to the maintenance, gain or loss of confirmed candidate miRNA genes. Additionally, one of the mechanisms that is part of the immune response to septic injury is an effective wound healing response. Wound closure after septic injury is critical in bacterial immobilization and in limiting haemolymph loss[2]. Hence, assessing wound healing efficiency (aseptic pricking) in miRNA deletion backgrounds is of crucial importance, since impaired wound closure can contribute greatly to the presence of false positives in our dataset.

All together, our results indicate that miRNA genes may differentially regulate the susceptibility to bacterial infection and the structure and cell density of haematopoietic tissues, targeting several immune-related genes. miRNA-mediated gene regulation requires sequence complementarity with the mRNA, therefore algorithms based on sequence similarity have been developed to define targets for miRNAs[56]. Predictions of miRNA-mRNA interactions are scattered around several databases and are generally based on sequence, physical-chemical properties, expression levels and/or experimental data[52]. Using one of the many available algorithms to predict such interactions, Fullaondo *et al*, 2012, performed an *in silico* screen for miRNAs involved in the immune response of *D. melanogaster*. According to their results, from a total of 176 miRNAs, 93 have assigned putative targets and from those 73 target transcripts with known roles in the immune response[57]. Our results reveal that all miRNA genes which reported significant differences in survival upon infection with *P. entomophila* and *P. putida* are in agreement with the predictions, targeting several cellular and humoral immune-related genes. However, assigning a biological function to a miRNA based only on predictive scores that list potential targets can be problematic and easily misinterpreted. Predictions that correlate miRNAs with immune-related genes are abundant and their

detection varies greatly in amount and accuracy depending on the algorithm used[42]. Furthermore, computational predictions can only suggest potential interactions, which may not be biologically relevant until proper functional validation is undertaken. Such caveat of the prediction of miRNA targets is important to take into consideration, particularly because some miRNA genes also include predicted high-score targets with annotated roles in general organismal physiology, which can impact survival in an infection context and influence the interpretation of our results. This highlights the necessity of further functional and molecular validation of miRNA-mRNA interactions, such as (1) analysis of target mRNA and protein levels in miRNA mutant backgrounds, (2) time and tissue specificity of the expression of all candidate miRNAs and their respective targets, (3) conditional expression of miRNA sponges (which are functionally equivalent to RNAi tools) and (4) overexpression of candidate miRNAs using UAS constructs.

4.2 The role of microRNAs in the systemic immunity of *D. melanogaster*

Deletion of mir-137 or mir-317 genes correlates with a consistently strong susceptibility to infection with both bacteria species, displaying significantly higher mortality rates when compared to their respective controls (Figure 3.1 and 3.2). This indicates that both miRNA genes are required for survival after bacterial infection, particularly with gram-negative bacteria, and possibly repress inhibitors of humoral defense mechanisms. According to the bioinformatic retrieval of mRNA targets, both mir-137 and mir-317 target genes with annotated functions in the defense response against gram-negative bacteria and fungi, particularly in the gut (Table 3.1). Furthermore, mir-137 targets *kayak*, a component of the JNK pathway that functions as an inhibitor of the Imd pathway[58], and *PGRP-LB,* which downregulates the Imd pathway upon infection with gram-negative bacteria[59]. Considering that mir-137 may act as a repressor of one or both genes, deleting it would increase their products and lead to an exacerbated Imd attenuation and higher mortality upon gram-negative bacterial infection.

On the contrary, target retrieval for mir-317 highlights very few immune-related genes. One of those is *pellino*, a negative regulator of the Toll pathway[60]. This signalling cascade is preferentially activated in the presence of gram-positive bacteria, but synergistic activation with the Imd pathway has also been reported, particularly after septic injury[13]. Thus, in the context of mir-317 deletion, Toll signalling attenuation could have indirect implications in the effectiveness of the defense mechanisms against gram-negative bacteria. Noteworthy, the activation of the immune response involves a coordinated change in many physiological processes which have a multitude of ways of interfering with host survival[2,61]. Due to this aspect and the fact that immunity to infection does not simply imply getting rid of the causative agent, any mutants that affect general features of the fitness of flies tend to exhibit higher susceptibility to infection. This is valid not only for mutations which affect stress responses, but also wound healing or the rebalancing of energy resources, having implications on fertility and life span[61]. These categories of biological responses are important to consider when analyzing the immune response, since they may influence the observed results. Additionally, this can be emphasized by the fact that miRNAs are pleiotropic regulatory sequences: a single miRNA can target several mRNAs for silencing and each mRNA can be silenced by more than one miRNA, resulting in a broad effect on the protein content of cells. The fact that these two candidates might be regulating other physiological processes is highlighted by the presence of general cellular physiology targets among the retrieved lists (Supplementary Data – Table 4). This is particularly evident in the case of mir-317 deletion which also reports a significantly shorter lifespan[47]. As mentioned above, additional tests, namely aseptic pricking in mir-137 and mir-317 knock-out lines, will disentangle between direct (infection itself) and indirect effects, such as wound healing. Furthermore, other factors may also be tested such as resistance to desiccation or starvation, providing important information about the possible multiple origin of the observed increase in susceptibility.

In contrast, the deletion of the mir-100/let-7/mir-125 cluster showed consistently lower mortality upon infection with both *Pseudomonas* species, implicating a higher resistance or tolerance

(Figure 3.1 and 3.2). The retrieved targets of the three miRNAs belonging to this cluster include genes involved in the activation or inhibition of several pathways of the antimicrobial humoral defences (Table 3.1). This includes Toll and Imd, as well as JAK-STAT and JNK pathways, all of which could contribute to the observed outcome. Furthermore, according to Garbuzov and Tatar (2010), Ecdysone can prime *Drosophila* S2 cells to express let-7 and mir-125, and the first can modulate the expression of *Diptericin*, maintaining this AMP at basal levels in homeostasis[46]. Therefore, deleting let-7 could lead to an increase in the levels of *Diptericin*, which could be enough to reduce the mortality rates in a bacterial infection context. Importantly, uncontrolled activation of the immune response may cause more damage to host cells than a pathogen would (immune pathology) and this may also negatively impact host survival and fitness[62], as it is indicated by the remarkably short lifespan of the 100/let-7/125 cluster deficiency line[47]. However, analysis of let-7 targets performed in different databases failed to report evidence of the described interaction between let-7 and the 3'UTR of *Diptericin*, questioning the sufficiency of such interaction and even database update and prediction accuracy. A better disentanglement of necessity and sufficiency of the different immune pathways to produce this resistance/tolerance phenotype, in combination or separately, will be of crucial importance. Moreover, rather than just decreasing pathogen load (resistance), tolerance to infection implies reducing the negative impact of an infection on host fitness without directly affecting the pathogen burden[63]. Thus, assessing bacterial clearance ability, as well further dissecting the molecular function of these miRNA genes will be instrumental to fully understand the role of the mir-100/let-7/mir-125 cluster in immune response activation and function.

Notably, the mir-31b and mir-2b-1 deletion lines have so far revealed opposite tendencies between the two species of bacteria tested (Figure 3.1 and 3.2). In both cases, while there is an increased susceptibility to infection by *P. entomophila*, this difference is reversed upon infection with *P. putida*. Indeed, on both mutant contexts survival after infection with *P. putida* is increased in comparison to the controls. If such opponent dynamics are maintained after complete biological replication is achieved it could imply the existence of a trade-off between the responses to both bacterial species, where some mutations become beneficial in infections with one pathogen and detrimental with the other. The retrieved targets for mir-31b include genes that are necessary for the activation of the Imd pathway (*zfh-1* and *mask*) and negative regulators of the JNK pathway (*puc*), which is important for stress response upon infection. For mir-2b-1 the retrieved list encompasses genes also required for Imd signalling (*tab2*) and for the response to gram-positive and fungal infection (e.g. *psh*) (Table 3.1). However, further replication is necessary to understand if the immune response in these mutants is affected towards increased susceptibility in general or specific responses arise from infections with different pathogens, where the predicted targets may have important roles in regulating this putative trade-off.

4.3 microRNAs and the cellular defences of *D. melanogaster*

Focusing on the cellular component of the immune system of *D. melanogaster*, we observed that miRNAs contribute to the regulation of haematopoiesis, namely the correct establishment of haemocyte numbers and proportions. In general, our results indicate that mir-969, mir-980, mir-1 and mir-124 may play a regulatory role on properties such as haemocyte adhesion and proliferation, as well as crystal cell and lamellocyte differentiation (Figure 3.3 and Table 3.2).

The increase in plasmatocyte density, the most abundant haemocyte type, reported for mir-969 is the product of smaller sessile haemocyte clusters and average plasmatocyte numbers (Figure 3.3 and Supplementary Data – Figure 4 and 5). This can be indicative of altered adhesion properties: among plasmatocytes and/or between these cells and the dorsal subepidermis of the larval body. In fact, the predicted targets of mir-969 include genes implicated in cell adhesion such as *vav*, *gho* and *Abi* (Table 3.1). Disruption of cell adhesion dynamics due to the overexpression of these genes in a mir-969 dependent manner could lead to an increased adhesion between plasmatocytes and hence smaller

sessile haemocyte clusters. Furthermore, this should influence the numbers of crystal cells, since their transdifferentiation from plasmatocytes is positively correlated with the number of contacts between cells[48]. According to our results, crystal cell numbers report no differences (Supplementary Data – Figure 6), suggesting that their differentiation is limited, possibly due to the existence of a threshold of cell contacts above which crystal cell numbers stabilize. This could, in turn, be established by a feedback mechanism that inhibits the differentiation of crystal cells in a context of exacerbated plasmatocyte adhesion. In this case, it is important to analyze the distance between nuclei, which is expected to decrease if plasmatocyte-to-plasmatocyte adhesion is deregulated. Moreover, because the establishment of crystal cell proportions also depends on the lasting stability of cell contacts, analyzing the *in vivo* rates of cell exchange between the sessile and circulating haemocyte compartments can also provide important information and be highly influenced by the adhesion between cells of the sessile clusters.

In contrast, mir-124 deletion shows a decrease in plasmatocyte density, resulting from a small reduction in plasmatocyte numbers and normal cluster size (Figure 3.3 and Supplementary Data – Figure 4 to 6). Such changes may be due to altered proliferation and apoptosis rates of these cells, impaired homing and/or defective adhesion of plasmatocytes to the epidermis. Notably, the retrieved list of targets for mir-124 is highly enriched in genes related to cell adhesion and migration (Table 3.2). Disrupting the achievement of the correct plasmatocyte numbers should also influence crystal cell numbers, which depend on plasmatocyte density to transdifferentiate. However, crystal cell numbers report no significant differences (Supplementary Data – Figure 6). This suggests that, either plasmatocyte adhesion to the epidermis is more sensitized to larval handling, and/or homing to the sessile clusters is impaired, and/or exchange rates between the sessile and circulating haemocyte compartments are higher, without impacting the numbers of crystal cells. Based on this, further estimation of the number of cell contacts and distance between nuclei is important to explain the maintenance of cluster size while reducing the number of plasmatocytes. Additionally, since the sessile compartment contributes greatly with haemocytes to circulation[23], assessing the number of plasmatocytes in circulation and cell exchange rates is instrumental to understand if migration and adhesion to the dorsal sub epidermis is also influencing the observed outcome.

Furthermore, deletion of mir-1 reported, in heterozygosity, a significant decrease in crystal cell density, indicating that this miRNA gene may be involved in the differentiation of crystal cells. The reported differences were exclusively due to a reduction in the absolute numbers of crystal cells, since tissue size is similar to the control (Figure 3.3 and Supplementary Data – Figure 4 and 5). Furthermore, the transdifferentiation of crystal cells in the sessile haemocyte clusters is currently described as being mediated by Notch signalling and dependent on the numbers of plasmatocytes, which are stable in mir-1 knock-out line. This might serve as an indication that mir-1 does not alter crystal cell numbers by changing the precursor cell-type, but rather acts in the regulation of downstream steps of fate decision. Importantly, crystal cells are highly unstable cell types which frequently rupture, in response to injury and oxidative stress[64]. This can also influence crystal cell numbers and may be subject to mir-1 regulatory action. Notably, the predicted targets for mir-1 include several genes with known function in Notch signalling and crystal cell differentiation (Table 3.2). Future assessment of LG haematopoiesis and crystal cell numbers in the other haematopoietic compartments, as well as dissecting important steps throughout crystal cell differentiation and the process of melanization, is important to elucidate the function of mir-1.

Finally, deletion of mir-980 revealed a strong reduction in the density of both crystal cells and plasmatocytes (Figure 3.3 and 3.4). The reported differences result in almost absent sessile haemocyte clusters, where a small number of haemocytes is still attached to the dorsal subepidermal layer (Figure 3.5). This disruption of tissue structure creates difficulties in the measurement of tissue size and thus can bias the obtained density values. Regardless, our results for the absolute numbers of both cell types reveal a remarkable reduction, pointing to the idea that the maintenance of haemocytes in mir-

980 deletion line is severely disturbed. Together with the observation of melanotic nodules in the body cavity of larvae (indicative of the presence of lamellocytes and self-tissue encapsulation) we further detected that mir-980 deletion led to ectopic lamellocyte differentiation (Figure 3.5). This differentiation event begins after the second larval instar and the phenotype is aggravated until the onset of pupation, where melanotic nodules are detected in large numbers. Such deregulation of the differentiation of lamellocytes indicates that mir-980 plays a role in homeostasis in keeping these cells undifferentiated. Among the several targets of mir-980, we found components of the JAK-STAT pathway such as *domeless* (*dome*) (Table 3.2). Domeless (Dome) is a transmembrane receptor necessary for the activation of the JAK-STAT pathway. In homeostasis, the activation of JAK-STAT signalling in the medullary zone of the LG prevents haemocyte differentiation, while in the sessile and circulating compartments it is required and sufficient to differentiate lamellocytes in response to tumours and parasitic wasp infestation[15]. In fact, *dome* is one of the many genes that are upregulated in larvae after parasitoid wasp infection[65]. We therefore hypothesize that, since mir-980 targets *dome* mRNA for degradation or destabilization, deleting this miRNA gene might lead to an increase in levels of Dome throughout the larval body. Increasing Dome amount could be enough to trigger JAK-STAT activation, which is determined by the proportion between the receptor and its antagonist *lat*, and lead to an ectopic lamellocyte differentiation and to the formation of melanotic tumours[12]. Our preliminary results using a GFP reporter for JAK-STAT activation indicate that deleting mir-980 leads to changes in the activation pattern of this pathway (Figure 3.6). The observed changes are not haemocyte specific and are localized to more widespread tissues in the larval body, which could include the fat body, the epidermis or even the muscles. In fact, a recent study has shown that parasitoid wasp infection leads to JAK-STAT activation in the larval muscles, which is mediated by circulating haemocytes and Upd cytokines[29]. Such activation in turn leads to the differentiation of lamellocytes and successful egg encapsulation[29]. A detailed assessment of which tissue is at the origin of the putative JAK-STAT activation, together with the analysis of the effects of *dome* overexpression is important to understand *dome* sufficiency and the role of mir-980 in regulating the levels of this receptor. Moreover, analysing if mir-980 is sufficient to rescue lamellocyte differentiation in a *dome* mutant context should shed light onto the importance of this putative regulatory interaction for the differentiation of lamellocytes.

It was originally thought that an interdependent action of the cellular and humoral components of the immune response of *D. melanogaster* was necessary to fight bacterial infection, especially due to the phagocytic properties of plasmatocytes. It is currently established that larval plasmatocytes are necessary for the activation of AMP production by the fat body in the context of oral infection. In adults, plasmatocyte ablation increases susceptibility to systemic bacterial infection. However, these cells are not required for the activation of Toll and Imd pathways[32,33]. Our results indicate that mir-980 deletion, for instance, causes a decrease in the number of plasmatocytes and crystal cells but shows no evidence of a defective systemic immune response in adults. On the other hand, the deletion of mir-124 reports lower plasmatocyte numbers and a higher susceptibility to bacterial infection (Figure 3.1 and 3.3). Assessing how miRNA deletions that lead to defects in survival to infection are correlated with deregulated proliferation and differentiation of haemocytes, or vice-versa, will also provide important evidence towards the disentanglement of the role of cellular and humoral components in the neutralization and elimination of pathogens.

Bibliography

1. Hoffmann, J. A. & Reichhart, J.-M. Drosophila innate immunity: an evolutionary perspective. *Nat. Immunol.* **3,** 121–126 (2002).
2. Lemaitre, B. & Hoffmann, J. The host defense of Drosophila melanogaster. *Annu. Rev. Immunol.* **25,** 697–743 (2007).
3. Kounatidis, I. & Ligoxygakis, P. Drosophila as a model system to unravel the layers of innate immunity to infection. *Open Biol.* **2,** 120075–120075 (2012).
4. Ferrandon, D., Imler, J.-L., Hetru, C. & Hoffmann, J. a. The Drosophila systemic immune response: sensing and signalling during bacterial and fungal infections. *Nat. Rev. Immunol.* **7,** 862–74 (2007).
5. Leulier, F. *et al.* The Drosophila immune system detects bacteria through specific peptidoglycan recognition. *Nat. Immunol.* **4,** 478–484 (2003).
6. Buchon, N., Silverman, N. & Cherry, S. Immunity in Drosophila melanogaster - from microbial recognition to whole-organism physiology. *Nat. Rev. Immunol.* **14,** 797 (2014).
7. Kleino, A. & Silverman, N. The Drosophila IMD pathway in the activation of the humoral immune response. *Dev. Comp. Immunol.* **42,** 25–35 (2014).
8. Silverman, N. *et al.* Immune activation of NF-kappaB and JNK requires Drosophila TAK1. *J. Biol. Chem.* **278,** 48928–48934 (2003).
9. Boutros, M., Agaisse, H. & Perrimon, N. Sequential activation of signaling pathways during innate immune responses in Drosophila. *Dev. Cell* **3,** 711–722 (2002).
10. Kallio, J. *et al.* Functional analysis of immune response genes in Drosophila identifies JNK pathway as a regulator of antimicrobial peptide gene expression in S2 cells. *Microbes Infect.* **7,** 811–819 (2005).
11. Myllymäki, H. & Rämet, M. JAK/STAT Pathway in Drosophila Immunity. *Scand. J. Immunol.* **79,** 377–385 (2014).
12. Agaisse, H., Perrimon, N., Agaisse, H. & Perrimon, N. The roles of JAK/STAT signaling in Drosophila immune responses. *Immunol. Rev.* **198,** 72–82 (2004).
13. Tanji, T., Hu, X., Weber, A. N. R. & Ip, Y. T. Toll and IMD pathways synergistically activate an innate immune response in Drosophila melanogaster. *Mol. Cell. Biol.* **27,** 4578–88 (2007).
14. Holz, A., Bossinger, B., Strasser, T., Janning, W. & Klapper, R. The two origins of hemocytes in Drosophila. *Development* **130,** 4955–62 (2003).
15. Honti, V., Csordás, G., Kurucz, É., Márkus, R. & Andó, I. The cell-mediated immunity of Drosophila melanogaster: Hemocyte lineages, immune compartments, microanatomy and regulation. *Dev. Comp. Immunol.* **42,** 47–56 (2014).
16. Vlisidou, I. & Wood, W. Drosophila blood cells and their role in immune responses. *FEBS J.* **282,** 1368–1382 (2015).
17. Evans, C. J., Hartenstein, V. & Banerjee, U. Thicker Than Blood : Conserved Mechanisms in Drosophila and Vertebrate Hematopoiesis. **5,** 673–690 (2003).
18. Crozatier, M. & Vincent, A. Drosophila: a model for studying genetic and molecular aspects of haematopoiesis and associated leukaemias. *Dis. Model. Mech.* **4,** 439–45 (2011).
19. Parsons, B. & Foley, E. Cellular immune defenses of Drosophila melanogaster. *Dev. Comp. Immunol.* **58,** 95–101 (2016).
20. Leitão, A. B. & Sucena, É. Drosophila sessile hemocyte clusters are true hematopoietic tissues that regulate larval blood cell differentiation. *Elife* **2015,** 1–38 (2015).
21. Krzemień, J. *et al.* Control of blood cell homeostasis in Drosophila larvae by the posterior signalling centre. *Nature* **446,** 325–328 (2007).
22. Jung, S.-H., Evans, C. J., Uemura, C. & Banerjee, U. The Drosophila lymph gland as a developmental model of hematopoiesis. *Development* **132,** 2521–33 (2005).
23. Babcock, D. T. *et al.* Circulating blood cells function as a surveillance system for damaged tissue in Drosophila larvae. *Proc. Natl. Acad. Sci. U. S. A.* **105,** 10017–22 (2008).
24. Gantier, M. P., Sadler, A. J. & Williams, B. R. G. Fine-tuning of the innate immune response by microRNAs. *Immunol. Cell Biol.* **85,** 458–462 (2007).
25. Ghosh, S., Singh, A., Mandal, S. & Mandal, L. Active Hematopoietic Hubs in Drosophila Adults Generate Hemocytes and Contribute to Immune Response. *Dev. Cell* 1–11 (2015).

doi:10.1016/j.devcel.2015.03.014
26. Márkus, R. *et al.* Sessile hemocytes as a hematopoietic compartment in Drosophila melanogaster. *Proc. Natl. Acad. Sci. U. S. A.* **106,** 4805–9 (2009).
27. Márkus, R., Kurucz, É., Rus, F. & Andó, I. Sterile wounding is a minimal and sufficient trigger for a cellular immune response in Drosophila melanogaster. *Immunol. Lett.* **101,** 108–111 (2005).
28. Morin-Poulard, I., Vincent, A. & Crozatier, M. The Drosophila JAK-STAT pathway in blood cell formation and immunity. *Jak-Stat* **2,** e25700 (2013).
29. Yang, H., Kronhamn, J., Ekström, J.-O., Korkut, G. G. & Hultmark, D. JAK / STAT signaling in Drosophila muscles controls the cellular immune response against parasitoid infection. *EMBO Rep.* **16,** 1–9 (2015).
30. Anderl, I. *et al.* Transdifferentiation and Proliferation in Two Distinct Hemocyte Lineages in Drosophila melanogaster Larvae after Wasp Infection. *PLOS Pathog.* **12,** e1005746 (2016).
31. Letourneau, M. *et al.* Drosophila hematopoiesis under normal conditions and in response to immune stress. *FEBS Lett.* (2016). doi:10.1002/1873-3468.12327
32. Charroux, B. & Royet, J. Elimination of plasmatocytes by targeted apoptosis reveals their role in multiple aspects of the Drosophila immune response. *Proc. Natl. Acad. Sci. U. S. A.* **106,** 9797–9802 (2009).
33. Defaye, A. *et al.* Genetic ablation of Drosophila phagocytes reveals their contribution to both development and resistance to bacterial infection. *J. Innate Immun.* **1,** 322–334 (2009).
34. Bushati, N. & Cohen, S. M. microRNA functions. *Annu Rev Cell Dev Biol* **23,** 175–205 (2007).
35. Shenoy, A. & Blelloch, R. H. Regulation of microRNA function in somatic stem cell proliferation and differentiation. *Nat. Rev. Mol. Cell Biol.* **15,** 565–576 (2014).
36. Bartel, D. P., Lee, R. & Feinbaum, R. MicroRNAs : Genomics , Biogenesis , Mechanism , and Function. *Cell* **116,** 281–297 (2004).
37. Wang, Y., Luo, J., Zhang, H. & Lu, J. microRNAs in the same clusters evolve to coordinately regulate functionally related genes. *Mol. Biol. Evol.* (2016). doi:10.1093/molbev/msw089
38. Han, J. *et al.* The Drosha-DGCR8 complex in primary microRNA processing. *Genes Dev.* **18,** 3016–27 (2004).
39. Ebert, M. S. & Sharp, P. a. Roles for MicroRNAs in conferring robustness to biological processes. *Cell* **149,** 505–524 (2012).
40. Brennecke, J., Hipfner, D. R., Stark, A., Russell, R. B. & Cohen, S. M. bantam encodes a developmentally regulated microRNA that controls cell proliferation and regulates the proapoptotic gene hid in Drosophila. *Cell* **113,** 25–36 (2003).
41. Wienholds, E. & Plasterk, R. H. a. MicroRNA function in animal development. *FEBS Lett.* **579,** 5911–5922 (2005).
42. Lodish, H. F., Zhou, B., Liu, G. & Chen, C.-Z. Micromanagement of the immune system by microRNAs. *Nat. Rev. Immunol.* **8,** 120–130 (2008).
43. O'Connell, R. M., Rao, D. S., Chaudhuri, A. a. & Baltimore, D. Physiological and pathological roles for microRNAs in the immune system. *Nat. Rev. Immunol.* **10,** 111–122 (2010).
44. Hussain, M. & Asgari, S. MicroRNAs as mediators of insect host-pathogen interactions and immunity. *J. Insect Physiol.* **70,** 151–158 (2014).
45. Choi, I. K. & Hyun, S. Conserved microRNA miR-8 in fat body regulates innate immune homeostasis in Drosophila. *Dev. Comp. Immunol.* **37,** 50–54 (2012).
46. Garbuzov, A. & Tatar, M. Hormonal regulation of drosophila microRNA let-7 and miR-125 that target innate immunity. *Fly (Austin).* **4,** (2010).
47. Chen, Y. *et al.* Resource Systematic Study of Drosophila MicroRNA Functions Using a Collection of Targeted Knockout Mutations. *Dev. Cell* **31,** 784–800 (2014).
48. Castanho, A. & Leitão, B. Hematopoiesis in the Drosophila larva : beyond the lymph gland. (2014).
49. Schindelin, J. *et al.* Fiji: an open-source platform for biological-image analysis. *Nat. Methods* **9,** 676–82 (2012).
50. Byun, J. *et al.* Automated tool for the detection of cell nuclei in digital microscopic images : Application to retinal images. *Mol. Vis.* (2006).
51. Grishagin, I. V. Automatic cell counting with ImageJ. *Anal. Biochem.* **473,** 63–65 (2015).
52. Tabas-Madrid, D. *et al.* Improving miRNA-mRNA interaction predictions. *BMC Genomics* **15 Suppl 1,** S2 (2014).

53. Minakhina, S. & Steward, R. Melanotic mutants in Drosophila: Pathways and phenotypes. *Genetics* **174,** 253–263 (2006).
54. Vodovar, N. *et al.* Complete genome sequence of the entomopathogenic and metabolically versatile soil bacterium Pseudomonas entomophila. *Nat. Biotechnol.* **24,** 673–679 (2006).
55. Martins, N. E., Faria, V. G., Teixeira, L., Magalhães, S. & Sucena, É. Host Adaptation Is Contingent upon the Infection Route Taken by Pathogens. *PLoS Pathog.* **9,** (2013).
56. Rajewsky, N. microRNA target predictions in animals. *Nat. Genet.* **38 Suppl,** S8-13 (2006).
57. Fullaondo, A. & Lee, S. Y. Identification of putative miRNA involved in Drosophila melanogaster immune response. *Dev. Comp. Immunol.* **36,** 267–273 (2012).
58. Kleino, A. *et al.* Inhibitor of apoptosis 2 and TAK1-binding protein are components of the Drosophila Imd pathway. *EMBO J.* **24,** 3423–34 (2005).
59. Zaidman-Rémy, A. *et al.* The Drosophila Amidase PGRP-LB Modulates the Immune Response to Bacterial Infection. *Immunity* **24,** 463–473 (2006).
60. Ji, S. *et al.* Cell-surface localization of Pellino antagonizes Toll-mediated innate immune signalling by controlling MyD88 turnover in Drosophila. *Nat. Commun.* **5,** 1–14 (2014).
61. Neyen, C., Bretscher, A. J., Binggeli, O. & Lemaitre, B. Methods to study Drosophila immunity. *Methods* **68,** 116–128 (2014).
62. Schneider, D. S. How and Why Does a Fly Turn Its Immune System Off? *PLoS Biol.* **5,** 1847–1849 (2007).
63. Medzhitov, R., Schneider, D. S. & Soares, M. P. Disease Tolerance as a Defense Strategy. *Science (80-.).* **335,** 936–941 (2012).
64. Bidla, G., Dushay, M. S. & Theopold, U. Crystal cell rupture after injury in Drosophila requires the JNK pathway, small GTPases and the TNF homolog Eiger. *J. Cell Sci.* **120,** 1209–1215 (2007).
65. Wertheim, B. *et al.* Genome-wide gene expression in response to parasitoid attack in Drosophila. *Genome Biol.* **6,** R94 (2005).

Supplementary Data

Supplementary Data – Figure 1– Crossing Scheme Representation

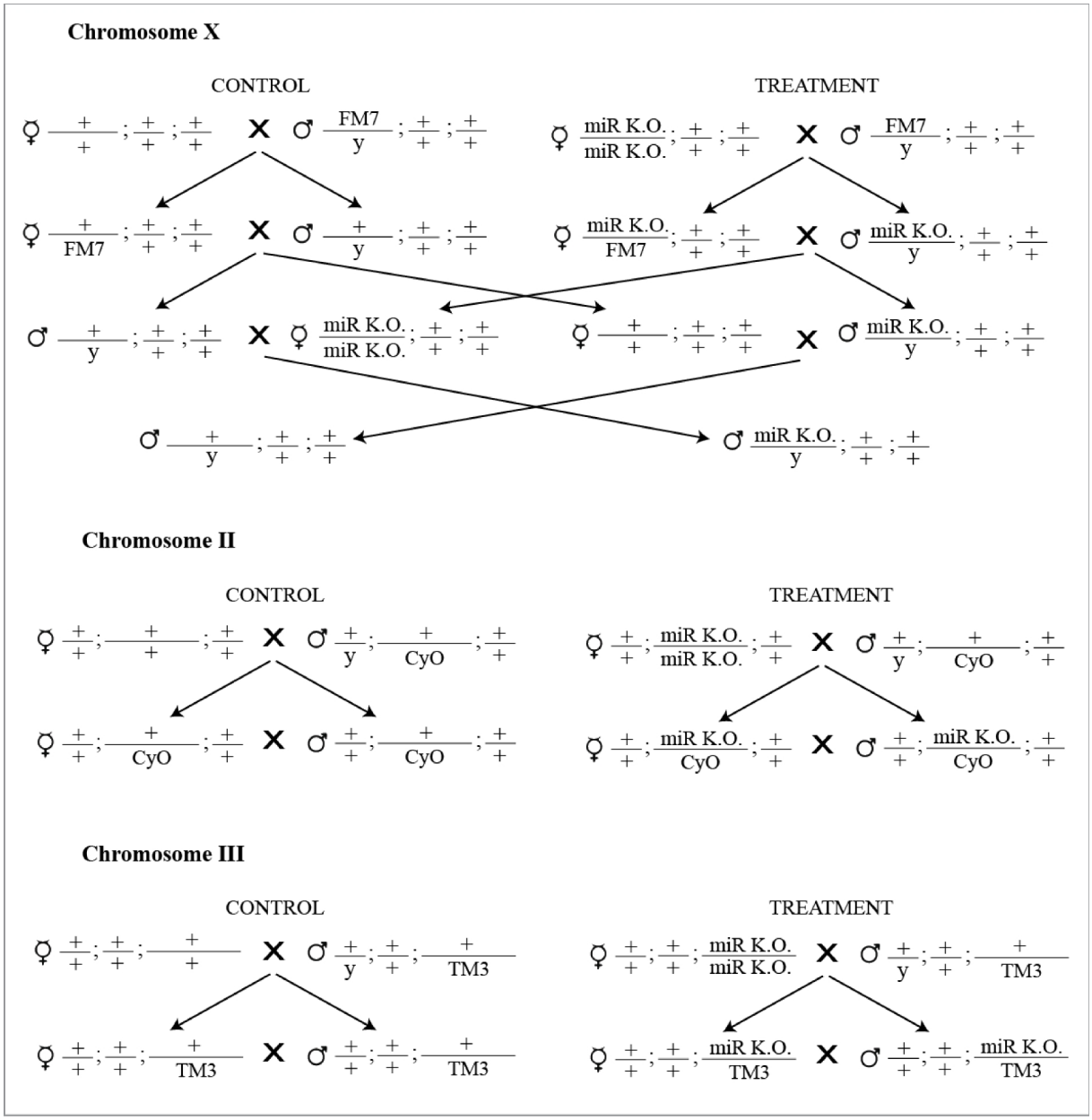

Supplementary Data - Figure 1 – Crossing Scheme Representation. Schematic representation of the crossing schemes performed to obtain the adult male flies that were included in the primary and secondary systemic immunity screens. Due to genetic background disparities, deletions located on the chromosome X were submitted to an extra generation of genetic background homogenization.

Supplementary Data - Table 1 - Collection of microRNA mutants		
miRNA	**Detailed Genotype**	**KO/KO Viability**
Control (X)	y[1]w[*]/FM7c, P{w[+mC]=GAL4-twi.G}108.4, P{UAS-2xEGFP}AX	1
Control (2)	w[1118]; + /CyO, P{w[+mC]=GAL4-twi.G}2.2, P{UAS-2xEGFP}AH2.2	1
Control (3)	w[1118]; +/+; + /TM3, P{Dfd-GMR-nvYFP}3, Sb[1]	1
mir-13b-2	y[1]w[*] TI{TI}mir-13b-2[KO]	1
mir-210	y[1]w[*] TI{w[+mW.hs]=GAL4}mir-210[KO]	1
mir-283	w[*] TI{TI}mir-283[KO]	1
mir-304	w[*] TI{TI}mir-304[KO]	1
mir-31b	w[*] TI{TI}mir-31b[KO]	1
mir-927	y[1]w[*] TI{TI}mir-927[KO]	1
mir-969	w[*] TI{w[+mW.hs]=GAL4}mir-969[KO]	1
mir-970	w[*] TI{TI}mir-970[KO]	1
mir-971	w[*] TI{w[+mW.hs]=GAL4}mir-971[KO]	1
mir-972,973,974	Df(1)mir-972-973-974-KO, y[1]w[*] TI{w[+mW.hs]=GAL4}mir-972-973-974-KO	1
mir-975,976,977	Df(1)mir-975-976-977-KO, w[*] TI{w[+mW.hs]=GAL4}-mir-975-976-977-KO	1
mir-980	TI{TI}mir-980[KO] w[*]	1
mir-981	TI{TI}mir-981[KO] w[*]	1
mir-982,303	Df(1)mir-982-303-KO, w[*],TI{w[+mW.hs]=TI}mir-982-303-KO	1
mir-984,983-1,983-2	Df(1)mir-984-983-1-983-2-KO, w[*]	1
mir-1	w[*]; mir-1[KO]/CyO, P{w[+mC]=GAL4-twi.G}2.2, P{UAS-2xEGFP}AH2.2	0
mir-100,let-7,125	w[*]; Df(2L)let-7-C[KO1], TI{w[+m*]=TI}CG10283[K01]/CyO, P{w[+mC]=GAL4-twi.G}2.2, P{UAS-2xEGFP}AH2.2	0
mir-124	w[*]; TI{w[+mW.hs]=TI}mir-124[Delta177.w+]/CyO, P{w[+mC]=GAL4-twi.G}2.2, P{UAS-2xEGFP}AH2.2	0
mir-133	w[*]; TI{w[+mW.hs]=TI}mir-133[KO]	1
mir-137	w[*]; TI{w[+mW.hs]=TI}mir-137[KO]	1
mir-14	w[*]; mir-14[Delta1]/CyO, P{w[+mC]=GAL4-Kr.C}DC3, P{w[+mC]=UAS-GFP.S65T}DC7	0
mir-184	w[*]; TI{w[+mW.hs]=TI}mir-184[KO]	1
mir-263a	w[*]; TI{w[+mW.hs]=TI}bft[Delta263a]/CyO, P{w[+mC]=GAL4-twi.G}2.2, P{UAS-2xEGFP}AH2.2	0
mir-275,305	w[*]; Df(2L)mir-275-305-KO, TI{w[+mW.hs]=TI}mir-275-305-KO/CyO, P{w[+mC]=GAL4-twi.G}2.2, P{UAS-2xEGFP}AH2.2	0
mir-278	w[*]; TI{w[+mW.hs]=TI}mir-278[KO]	1
mir-281-1,281-2	w[*]; Df(2R)mir-281-1-281-2-KO	1
mir-2a-2,2a-1,2b-2	w[*]; Df(2L)mir-2a-2-2a-1-2b-2-KO	1
mir-2b-1	w[*]; TI{w[+mW.hs]=TI}mir-2b-1[KO]	1
mir-307-a,307-b	w[*]; Df(2R)mir-307a-307b-KO	1
mir-308	w[*]; TI{TI}mir-308[KO]/CyO, P{w[+mC]=GAL4-twi.G}2.2, P{UAS-2xEGFP}AH2.2	0
mir-309	w[*]; Df(2R)mir-309-6[Delta1], TI{w[+mW.hs]=GFP}Df-mir-309-6[Delta1]/CyO, P{w[+mC]=GAL4-twi.G}2.2, P{UAS-2xEGFP}AH2.2	0
mir-310,311,312,313	w[*]; Df(2R)mir-310-311-312-313 P{ry[+t7.2]=neoFRT}42D	1
mir-31a	w[*]; TI{w[+mW.hs]=TI}mir-31a[KO]	1
mir-375	w[*]; TI{w[+mW.hs]=GAL4}mir-375[KO]	1
mir-8	w[*]; mir-8[Delta2]/CyO, P{w[+mC]=GAL4-Kr.C}DC3, P{w[+mC]=UAS-GFP.S65T}DC7	0
mir-87	w[*]; TI{w[+mW.hs]=TI}mir-87[KO]	1
mir-932	w[*]; TI{TI}mir-932[KO]	1
mir-959,960,961,962	w[*]; Df(2L)mir-959-960-961-962-KO	1
mir-963, 964	w[*]; Df(2L)mir-963-964-KO/CyO, P{w[+mC]=GAL4-twi.G}2.2, P{UAS-2xEGFP}AH2.2	0
mir-965	w[*]; TI{TI}mir-965[KO]	1
mir-966	w[*]; TI{TI}mir-966[KO]	1
mir-967	w[*]; TI{TI}mir-967[KO]	1
mir-968,1002	w[*]; Df(2L)mir-968-1002-KO, TI{w[+mW.hs]=GAL4}mir-968-1002-KO	1
mir-986	w[*]; TI{TI}mir-986[KO]	1
mir-987	w[*]; TI{w[+mW.hs]=GAL4}mir-987[KO]	1
mir-988	w[*]; TI{TI}mir-988[KO]	1
mir-989	w[*]; TI{w[+mW.hs]=TI}mir-989[KO]	1
mir-990	w[*]; TI{TI}mir-990[KO]	1

Supplementary Data - Table 1 - Collection of microRNA mutants (continued)		
miRNA	**Detailed Genotype**	**KO/KO Viability**
mir-9c	w[*]; TI{TI}mir-9c[KO]	1
bantam	w[*]; Df(3L)ban[Delta1]/TM3, P{Dfd-GMR-nvYFP}3, Sb[1]	0
mir-10	w[*]; TI{w[+mW.hs]=GAL4}mir-10[KO]	1
mir-1000	w[*]; TI{TI}mir-1000[KO]/TM3, P{Dfd-GMR-nvYFP}3, Sb[1]	0
mir-1003	w[*]; TI{TI}mir-1003[KO]/TM3, P{Dfd-GMR-nvYFP}3, Sb[1]	0
mir-1010	w[*]; TI{TI}mir-1010[KO]/TM3, P{Dfd-GMR-nvYFP}3, Sb[1]	0
mir-1017	w[*]; TI{TI}mir-1017[KO]/TM3, P{Dfd-GMR-nvYFP}3, Sb[1]	0
mir-11	w[*]; TI{TI}-mir11[KO.w-]	1
mir-190	w[*]; TI{TI}mir-190[KO]/TM3, P{Dfd-GMR-nvYFP}3, Sb[1]	0
mir-193	w[*]; TI{w[+mW.hs]=GAL4}mir-193[KO]	1
mir-219	w[*]; TI{w[+mW.hs]=TI}mir-219[KO]	1
mir-252	w[*]; TI{TI}mir-252[KO]/TM3, P{Dfd-GMR-nvYFP}3, Sb[1]	0
mir-263b	w[*]; TI{TI}mir-263b[Delta]	1
mir-274	w[*]; TI{TI}mir-274[KO]	1
mir-276a	w[*]; TI{w[+mW.hs]=TI}mir-276a[KO]/TM3, P{Dfd-GMR-nvYFP}3, Sb[1]	0
mir-276b	w[*]; TI{TI}mir-276b[KO]/TM3, P{Dfd-GMR-nvYFP}3, Sb[1]	0
mir-277,34	w[*]; Df(3R)mir-277-34-KO, TI{w[+mW.hs]=TI}mir-277-34-KO/TM3, P{Dfd-GMR-nvYFP}3, Sb[1]	0
mir-282	w[*]; TI{w[+mW.hs]=TI}mir-282[KO]	1
mir-284	w[*]; TI{w[+mW.hs]=TI}mir-284[KO]	1
mir-285	w[*]; TI{w[+mW.hs]=TI}mir-285[KO]	1
mir-2c,13-a,13-b-1	w[*]; Df(3R)mir-2c-13a-13b-1-KO, TI{w[+mW.hs]=TI}mir-2c-13a-13b-1-KO	1
mir-314	w[*]; TI{w[+mW.hs]=TI}mir-314[KO]	1
mir-317	w[*]; TI{w[+mW.hs]=TI}mir-317[KO]	1
mir-33	w[*]; TI{TI}mir-33[KO]	1
mir-929	w[*]; TI{TI}mir-929[KO]	1
mir-92a	w[*]; TI{TI}mir-92a[KO]	1
mir-92b	w[*]; TI{w[+mW.hs]=TI}mir-92b[KO]	1
mir-955	w[*]; TI{w[+mW.hs]=GAL4}mir-955[KO]	1
mir-956	w[*]; TI{w[+mW.hs]=GAL4}mir-956[KO]	1
mir-957	w[*]; TI{w[+mW.hs]=TI}mir-957[KO]	1
mir-958	w[*]; TI{w[+mW.hs]=TI}mir-958[KO]	1
mir-994	w[*]; TI{w[+mW.hs]=TI}mir-994[KO]	1
mir-995	w[*]; TI{TI}mir-995[KO]/TM3, P{Dfd-GMR-nvYFP}3, Sb[1]	0
mir-999	w[*]; TI{TI}mir-999[KO]	1
mir-iab-4,iab-8	w;; Δmir-iab-4,iab-8/TM3, P{Dfd-GMR-nvYFP}3, Sb[1]	0

Supplementary Data - Table 1 – Collection of microRNA mutants. Description of the panel of microRNA knock-outs used to perform both systemic immunity and haematopoiesis surveys. Detailed genotype information is provided together with the viability of the homozygous state of each deletion (KO/KO Viability). Lines assigned with zero viability showed embryonic, larval or pupal lethality.

Supplementary Data - Table 2 - Summary of systemic immunity statistical analysis

Rank	miRNA	Survival Curves	Hazard Ratios			
		Logrank (Mantel-Cox)	Cox Model (Average)	Cox Model (Independent Replicates)		
1	mir-124	****	*	-	-	***
1	mir-137	***	*	***	-	**
1	mir-278	****	***	-	*	-
1	mir-281-1, 281-2	****	***	-	***	NA
1	mir-2b-1	****	***	-	***	-
1	mir-959, 960, 961, 962	****	***	-	***	-
1	mir-990	****	***	***	**	-
1	mir-284	****	***	-	-	*
1	mir-285	****	***	*	-	**
1	mir-955	****	***	-	**	-
1	mir-957	****	***	*	-	-
1	mir-929	****	**	**	NA	NA
1	mir-31b	****	**	-	-	-
1	mir-317	****	***	-	-	-
2	mir-100, let-7, 125	***	-	-	-	*
2	mir-310, 311, 312, 313	***	-	-	-	NA
3	mir-965	-	***	**	-	-
3	mir-92a	-	***	-	***	-
3	mir-999	-	***	-	-	-
3	mir-970	-	**	-	-	-
3	mir-971	-	**	-	-	-
3	mir-972, 973, 974	-	*	-	-	-
3	mir-11	-	***	-	-	-
3	mir-984, 983-1, 983-2	-	*	-	-	*
3	mir-375	-	*	-	*	NA
3	mir-987	-	***	***	-	NA
3	mir-10	-	**	-	-	-
3	mir-274	-	***	-	-	NA
3	mir-2c, 13-a, 13-b-1	-	***	*	-	-
3	mir-33	-	***	**	-	NA
3	mir-958	-	***	-	*	NA
3	mir-133	-	-	-	**	NA
3	mir-263a	-	-	-	**	-
3	mir-2a-2, 2a-1, 2b-2	-	-	-	*	-
3	mir-308	-	-	-	-	***
3	mir-963, 964	-	-	-	**	-
3	mir-967	-	-	-	**	-
3	mir-986	-	-	**	-	-
3	mir-9c	-	-	-	**	-
3	mir-1000	-	-	-	*	NA
3	mir-277, 34	-	-	-	*	-
3	mir-314	-	-	-	**	-
4	mir-iab-4,iab-8	-	-	-	-	NA
4	mir-13b-2	-	-	-	-	-
4	mir-210	-	-	-	-	-
4	mir-283	-	-	-	-	-
4	mir-304	-	-	-	-	-
4	mir-927	-	-	-	-	-
4	mir-969	-	-	-	-	-
4	mir-975, 976, 977	-	-	-	-	-
4	mir-980	-	-	-	-	-
4	mir-981	-	-	-	-	-
4	mir-982, 303	-	-	-	-	-

Supplementary Data - Table 2 - Summary of systemic immunity statistical analysis (continued)

Rank	miRNA	Survival Curves	Hazard Ratios			
		Logrank (Mantel-Cox)	Cox Model (Average)	Cox Model (Independent Replicates)		
4	mir-1	-	-	-	-	-
4	mir-14	-	-	-	-	NA
4	mir-184	-	-	-	NA	NA
4	mir-275, 305	-	-	-	-	-
4	mir-307-a, 307-b	-	-	-	-	-
4	mir-309	-	-	-	-	-
4	mir-31a	-	-	-	-	-
4	mir-8	-	-	-	-	-
4	mir-87	-	-	-	-	-
4	mir-932	-	-	-	-	-
4	mir-966	-	-	-	-	-
4	mir-968, 1002	-	-	-	-	-
4	mir-988	-	-	-	-	-
4	mir-989	-	-	-	-	-
4	bantam	-	-	-	-	-
4	mir-1003	-	-	-	-	-
4	mir-1010	-	-	-	-	-
4	mir-1017	-	-	-	-	-
4	mir-190	-	-	-	-	-
4	mir-193	-	-	-	-	-
4	mir-219	-	-	-	-	-
4	mir-252	-	-	-	NA	NA
4	mir-263b	-	-	-	-	-
4	mir-276a	-	-	-	-	NA
4	mir-276b	-	-	-	-	NA
4	mir-282	-	-	-	-	-
4	mir-92b	-	-	-	-	NA
4	mir-956	-	-	-	-	NA
4	mir-994	-	-	-	-	NA
4	mir-995	-	-	-	-	-

Rank	Definition
1	All statistical approaches detect differences.
2	Survival dynamics and hazard ratios at day six show significant differences, but no statistical difference is detected within individual biological replicates.
3	No differences are detected between survival dynamics, but hazard ratios at day six show significantly different results in bulk and/or separately.
4	No statistical differences are detected.

Supplementary Data - Table 2 – Summary of systemic immunity statistical analysis. Summarized results of the statistical analysis performed on the data obtained from the systemic immunity primary survey. NA designates missing replicates. **p-value* < 0,05; ***p-value* < 0,01 ; ****p-value* < 0,001 ; *****p-value* < 0,0001.

Supplementary Data – Figure 2 (A-G) – Systemic immunity primary screen survival curves

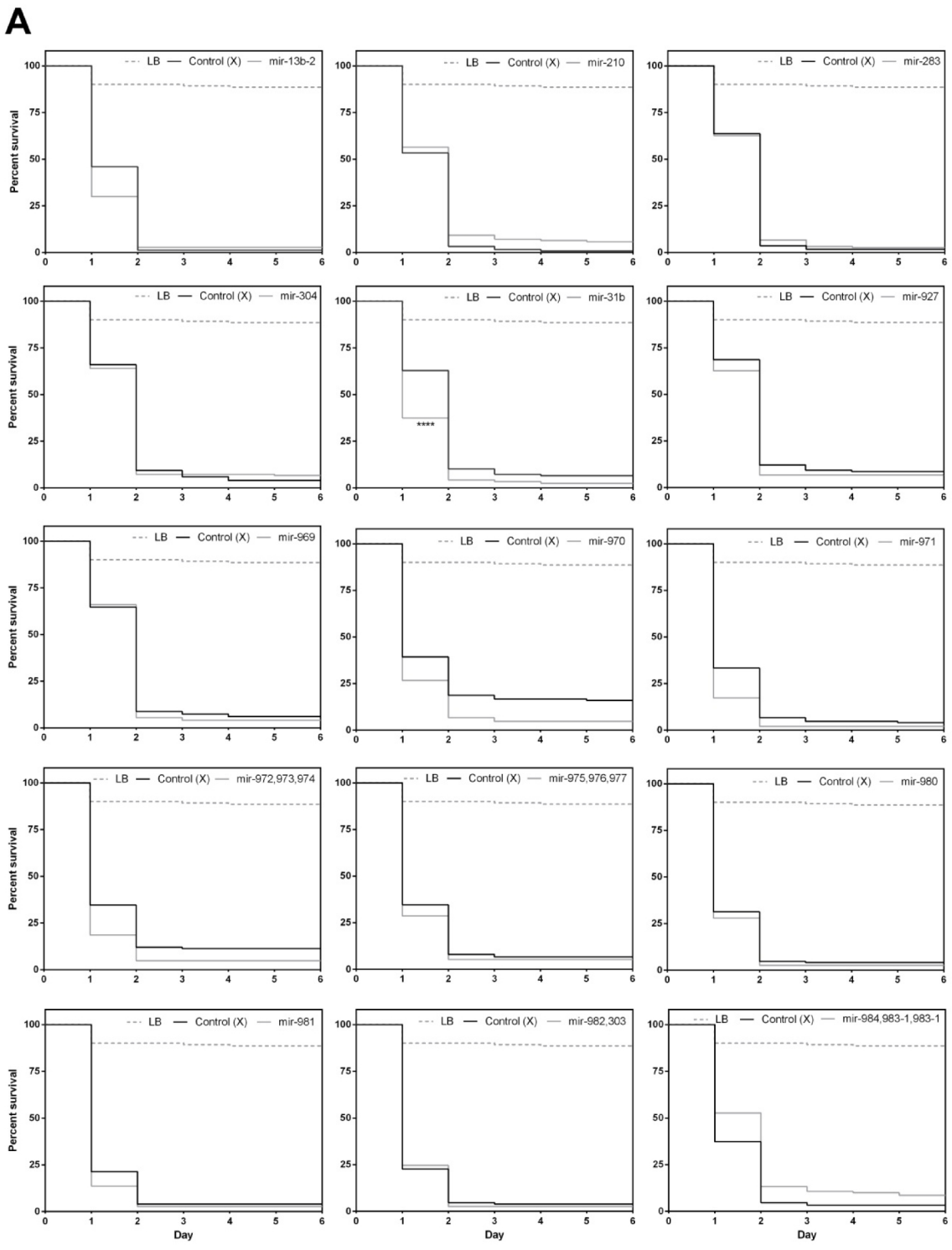

B

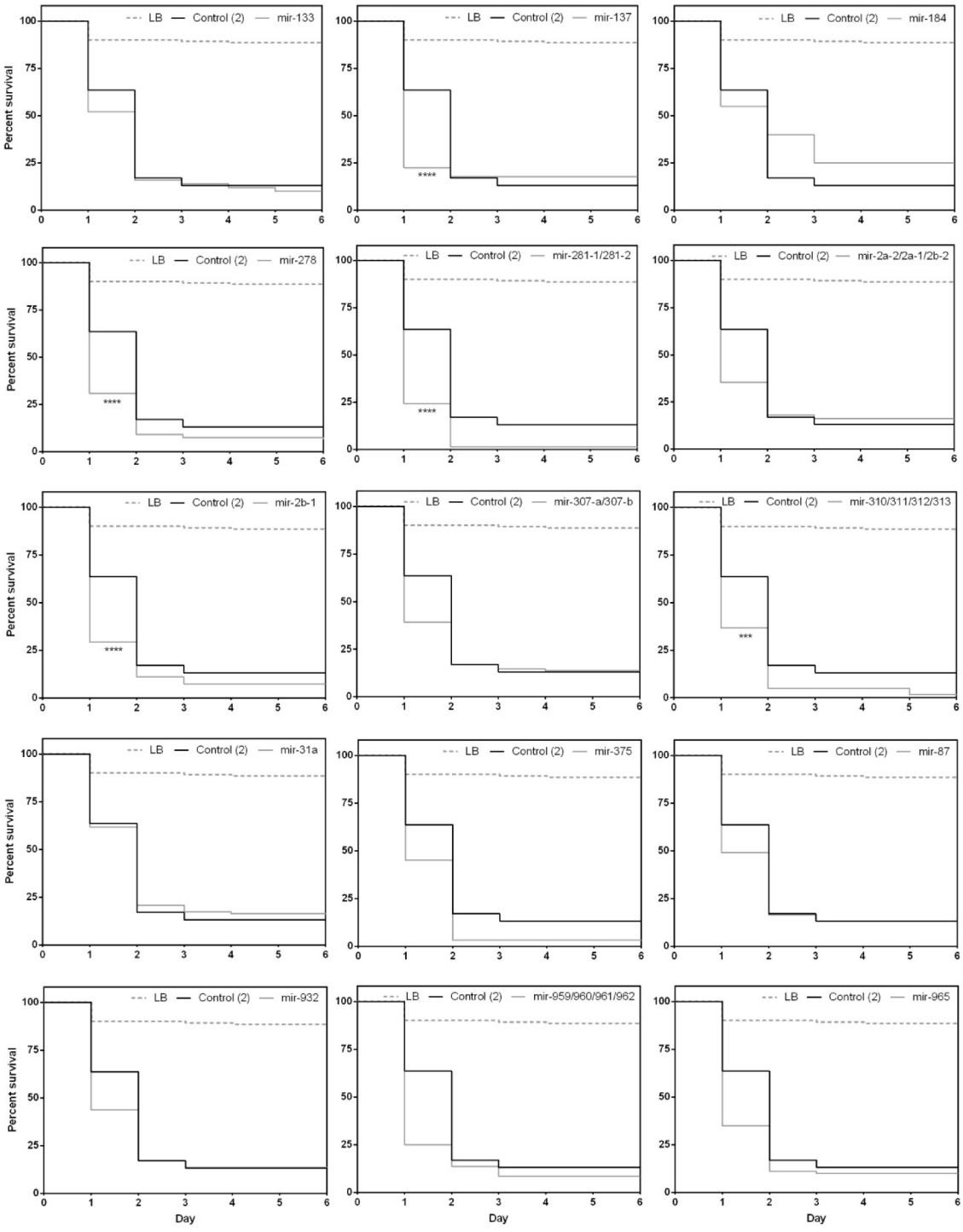
LB
Control (2)
mir-133
mir-137
mir-184
mir-278
mir-281-1/281-2
mir-2a-2/2a-1/2b-2
mir-2b-1
mir-307-a/307-b
mir-310/311/312/313
mir-31a
mir-375
mir-87
mir-932
mir-959/960/961/962
mir-965
Percent survival
Day
****
***

C

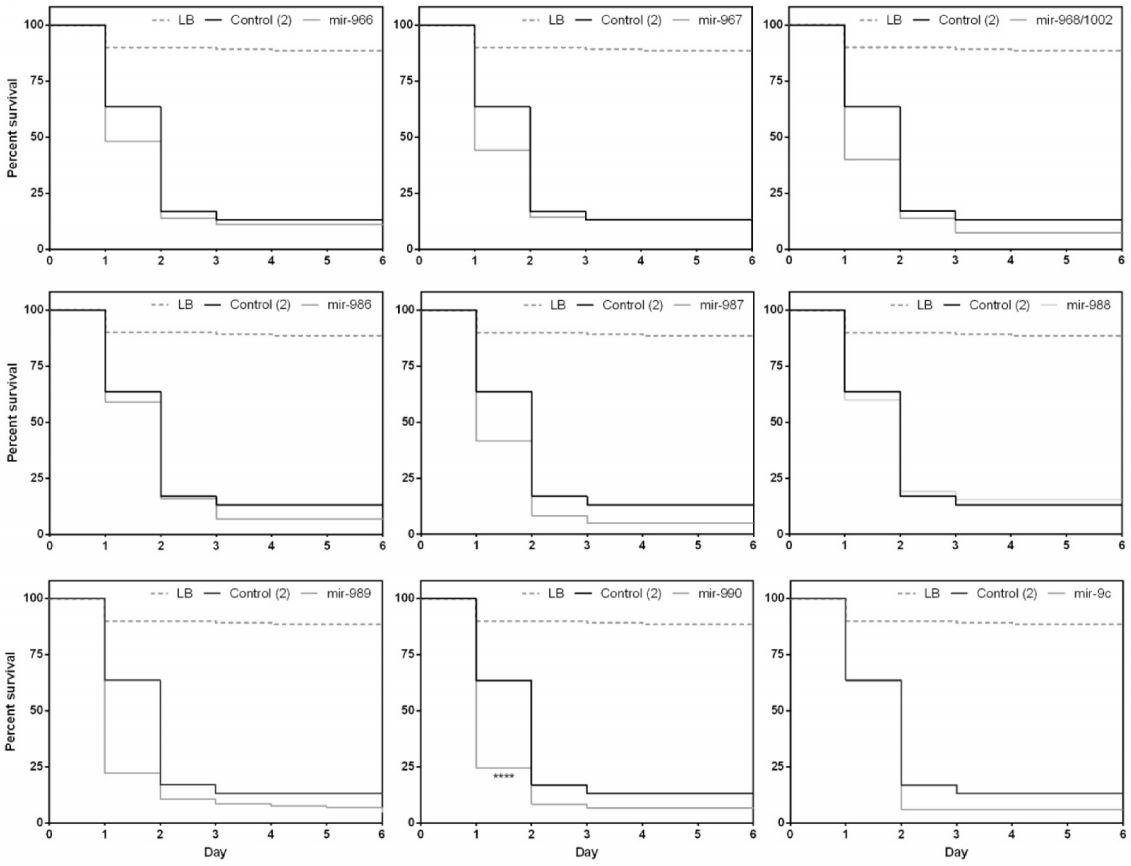
LB
Control (2)
mir-966
mir-967
mir-968/1002
mir-986
mir-987
mir-988
mir-989
mir-990
mir-9c
Percent survival
Day
****

D

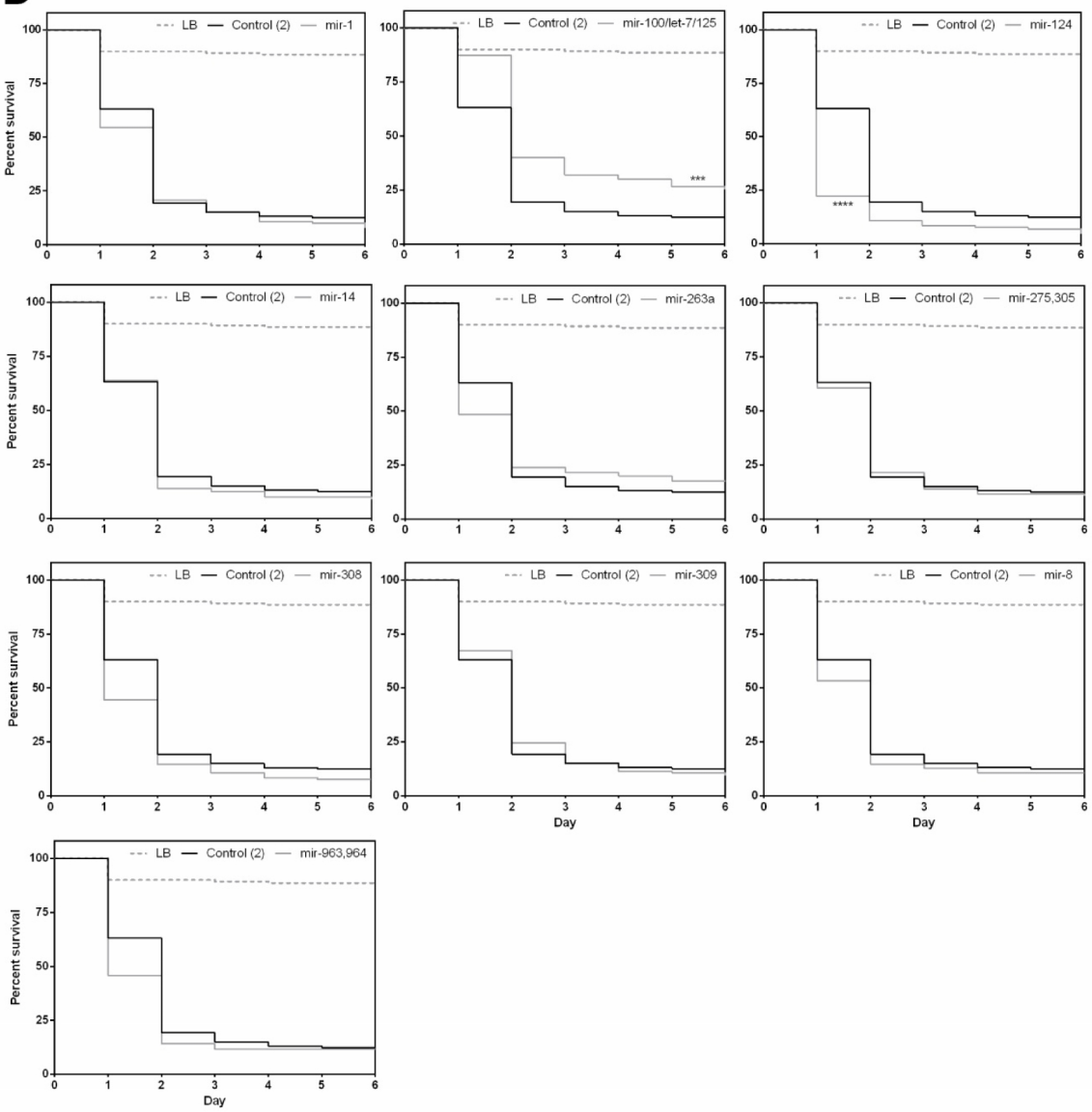
LB
Control (2)
mir-1
mir-100/let-7/125
mir-124
mir-14
mir-263a
mir-275,305
mir-308
mir-309
mir-8
mir-963,964
Percent survival
Day
***
****

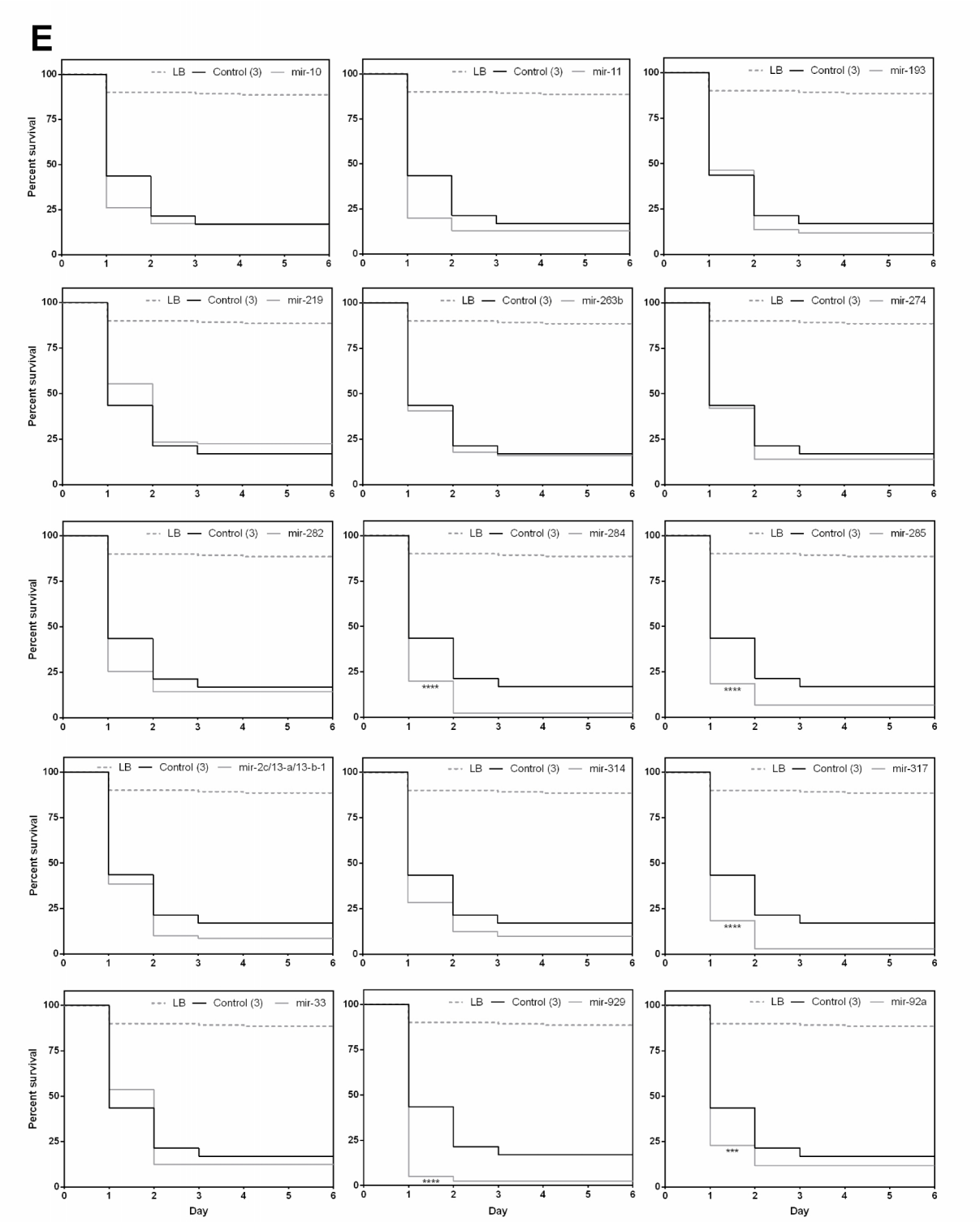
E
LB
Control (3)
mir-10
mir-11
mir-193
mir-219
mir-263b
mir-274
mir-282
mir-284
mir-285
mir-2c/13-a/13-b-1
mir-314
mir-317
mir-33
mir-929
mir-92a
Percent survival
Day
****
***

F

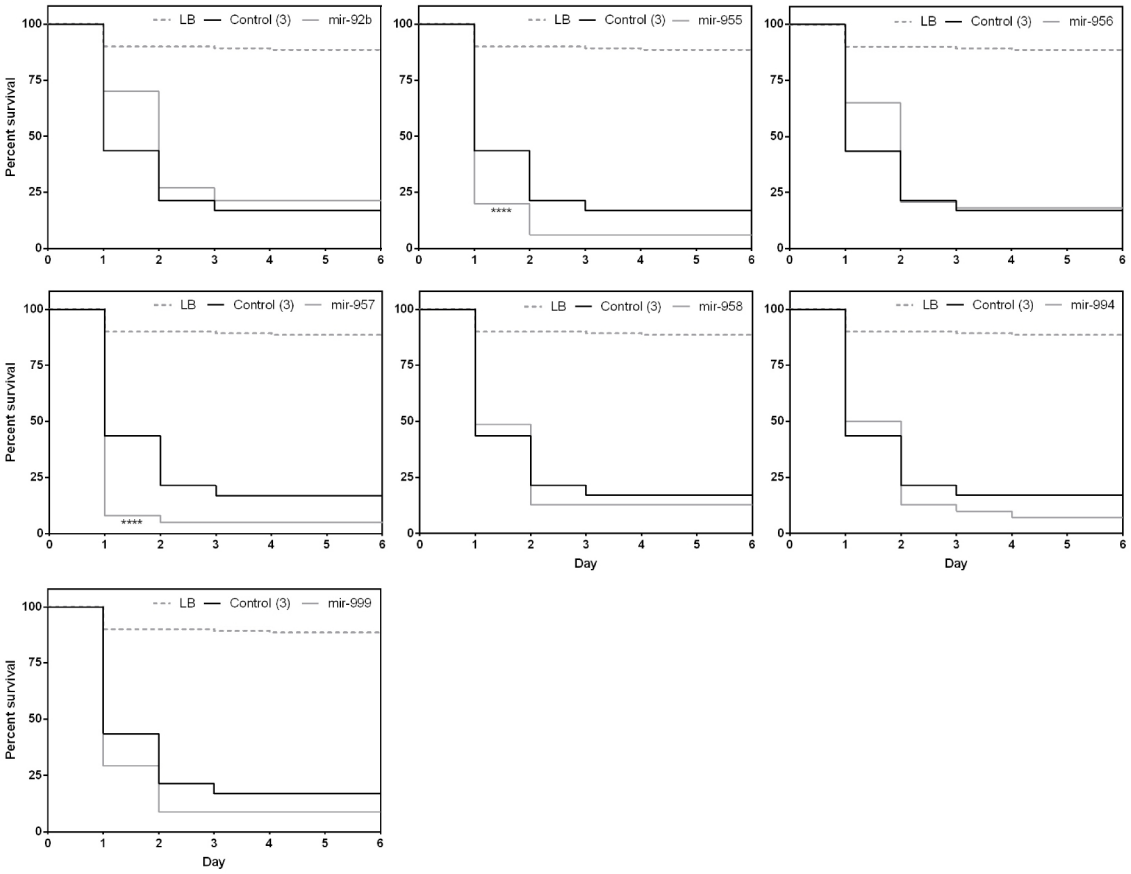
LB
Control (3)
mir-92b
mir-955
mir-956
mir-957
mir-958
mir-994
mir-999
Percent survival
Day
****

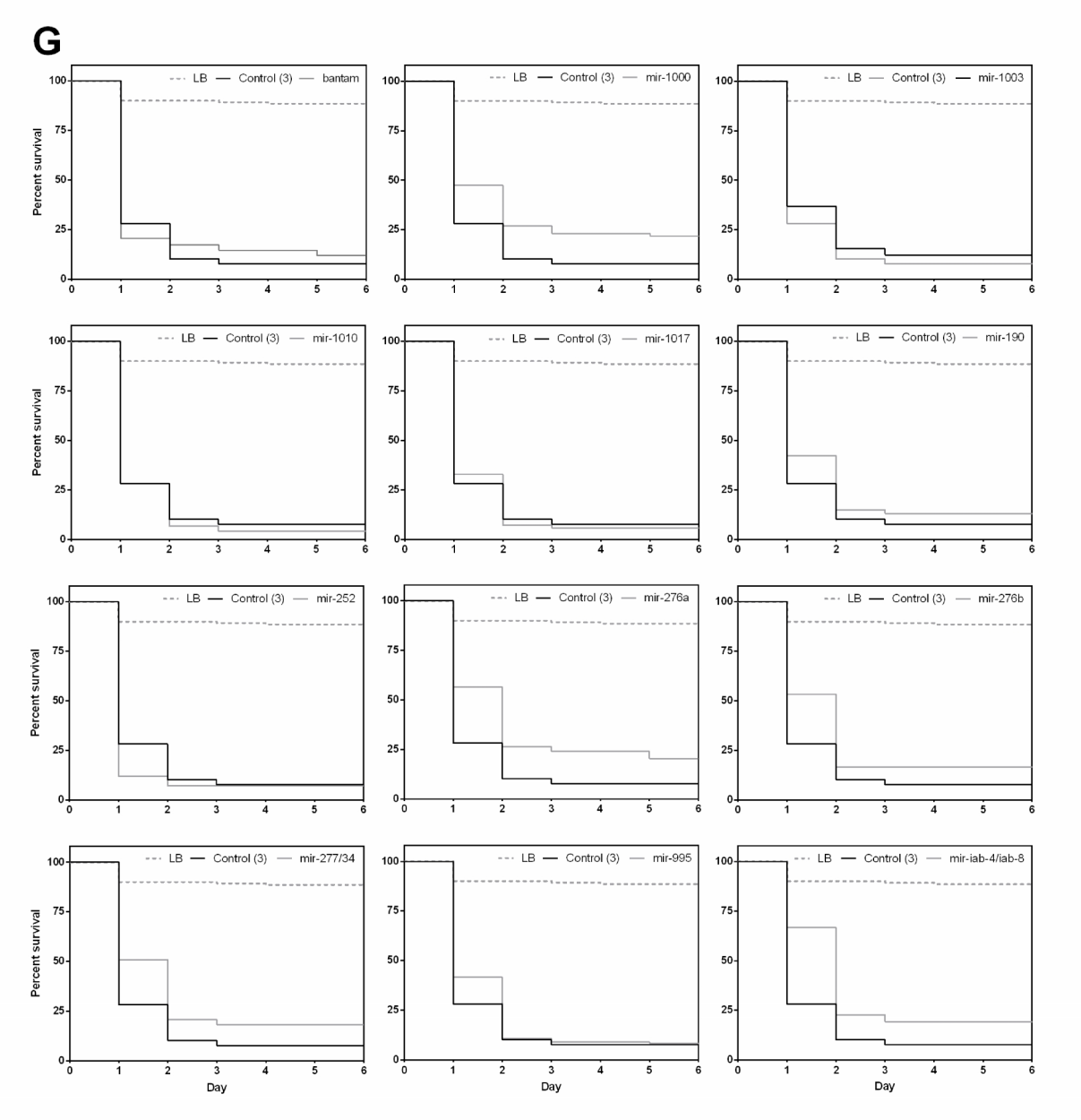

Supplementary Data – Figure 2 (**A-G**) – **Systemic immunity primary screen survival curves.** Survival curves obtained from the systemic immunity primary survey of microRNA knock-out lines infected with *P. entomophila* (See Materials and Methods). (**A**) microRNA knock-out lines located in the chromosome X. (**B-C**) Homozygous viable microRNA knock-out lines located in the chromosome II and (**E-F**) III. (**D**) Homozygous lethal microRNA knock-out lines located in the chromosome II and (**G**) III. **p-value* < 0,05; ***p-value* < 0,01 ; ****p-value* < 0,001 ; *****p-value* < 0,0001.

Supplementary Data - Table 3 - Summary of systemic immunity statistical analysis of microRNA candidate genes		
miRNA	**Survival Curves Logrank (Mantel-Cox)**	**Hazard Ratios Cox Model**
mir-31b	*	***
mir-100,let-7,125	****	***
mir-137	****	**
mir-2b-1	**	*
mir-317	****	***
mir-124	-	-
mir-278	-	-
mir-281-1,281-2	-	-
mir-310,311,312,313	-	-
mir-959,960,961,962	-	-
mir-990	-	-
mir-284	-	-
mir-285	-	-
mir-955	-	-
mir-957	-	-

Supplementary Data - Table 3 - Summary of systemic immunity statistical analysis of microRNA candidate genes. Summarized results of the statistical analysis performed on the data obtained from the systemic immunity secondary survey (See Materials and Methods). **p-value* < 0,05; ***p-value* < 0,01 ; ****p-value* < 0,001 ; *****p-value* < 0,0001.

Supplementary Data – Figure 3 – Systemic immunity survival curves of candidate microRNA genes.

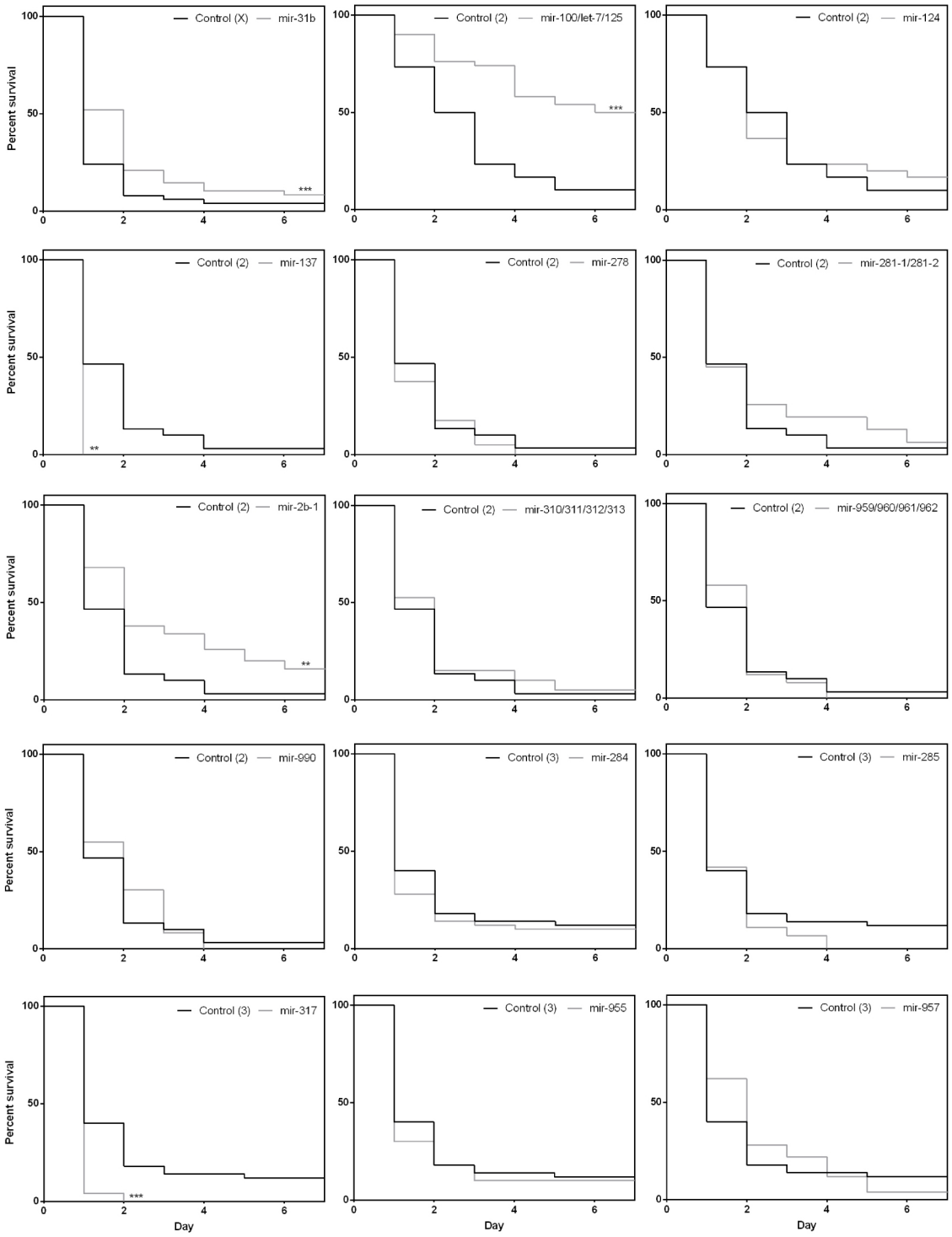

Supplementary Data – Figure 3 – Systemic immunity survival curves of candidate microRNA genes. Survival curves obtained from the systemic immunity secondary survey of microRNA knock-out lines infected with *P. putida* (See Materials and Methods). **p-value* < 0,05; ***p-value* < 0,01 ; ****p-value* < 0,001 ; *****p-value* < 0,0001.

Supplementary Data – Figure 4 – Sessile haemocyte clusters size.

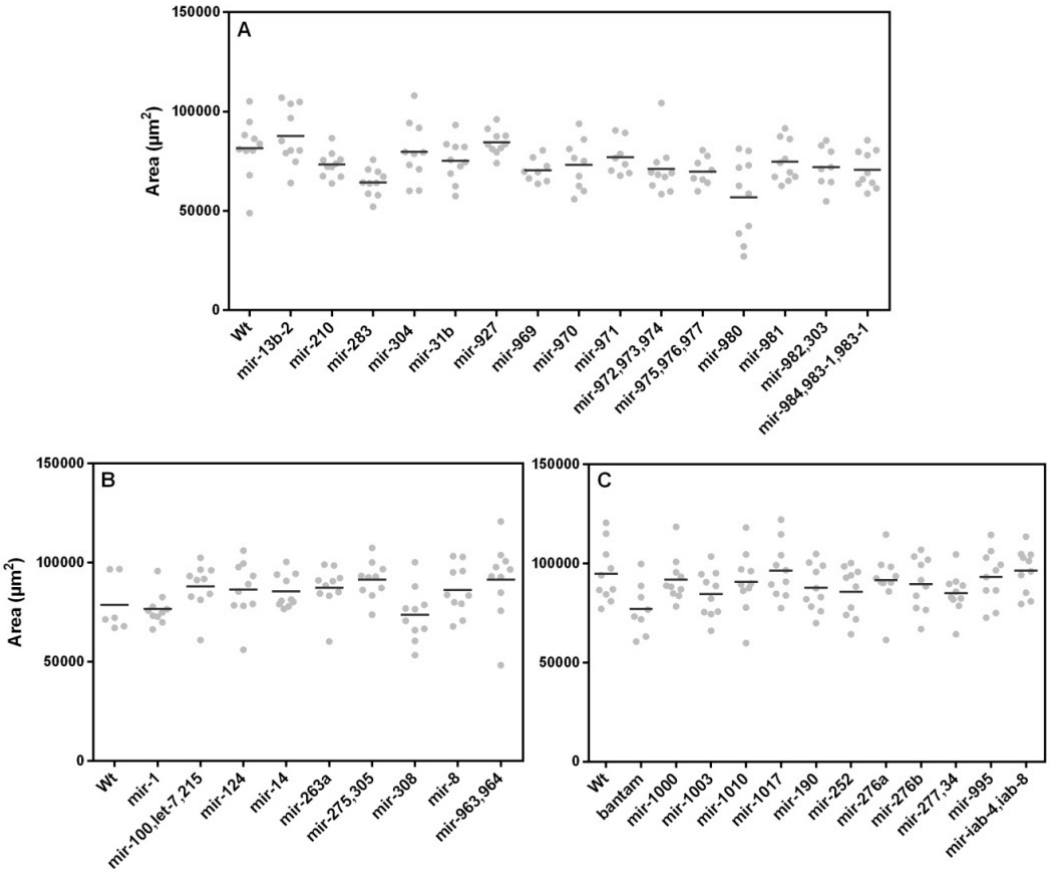

Supplementary Data – Figure 4 – Sessile haemocyte clusters size. Surface area of the most posterior sessile haemocyte cluster of L3 male larvae (µm^2). (**A**) Sessile haemocyte cluster size of microRNA knock-out lines located in the chromosome X. (**B**) Sessile haemocyte cluster size of homozygous lethal microRNA knock-out lines located in the chromosome II and (**C**) III. **p-value* < 0,05; ***p-value* < 0,01.

Supplementary Data – Figure 5 – Plasmatocyte numbers.

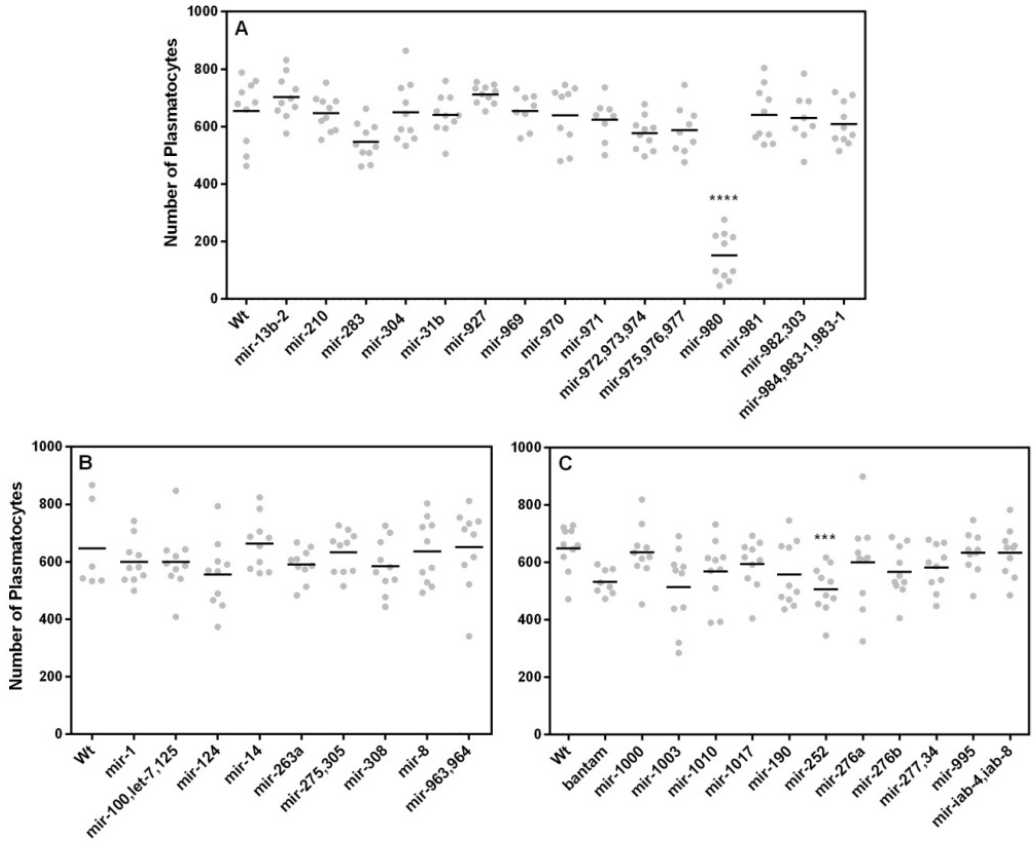

Supplementary Data – Figure 5 – Plasmatocyte numbers. Quantification of the absolute numbers of plasmatocytes in the most posterior sessile haemocyte cluster of L3 male larvae. (**A**) Plasmatocyte numbers of microRNA knock-out lines located in the X chromosome. (**B**) Plasmatocyte numbers of homozygous lethal microRNA knock-out lines located in the II chromosome and (**C**) III chromosome. **p-value* < 0,05; ***p-value* < 0,01 ; ****p-value* < 0,001 ; *****p-value* < 0,0001.

Supplementary Data – Figure 6 – Crystal cell numbers.

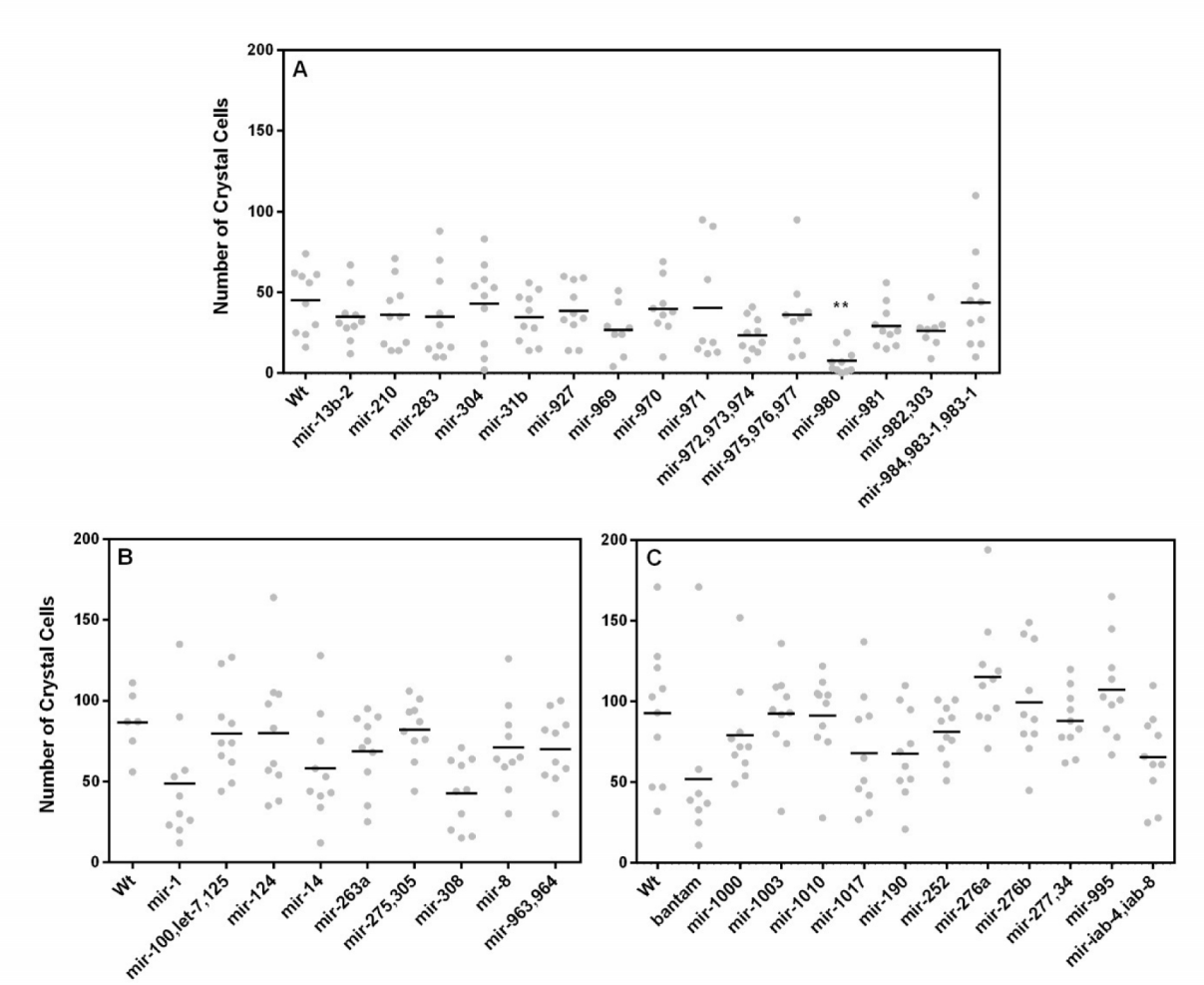

Supplementary Data – Figure 6 – Crystal cell numbers. Quantification of the absolute numbers of crystal cells in the most posterior sessile haemocyte cluster of L3 male larvae. (**A**) Crystal cell numbers of microRNA knock-out lines located in the X chromosome. (**B**) Crystal cell numbers of homozygous lethal microRNA knock-out lines located in the II chromosome and (**C**) III chromosome. **p-value* < 0,05; ***p-value* < 0,01.

Supplementary Data - Table 4 (A-K) - Summary of high-score targets of miRNA genes.

Detailed description of the first 200 retrieved targets for candidate miRNAs with roles in haematopoiesis or the systemic immune response, can be found at: https://drive.google.com/open?id=0B1FPzscYkjqjQ3ptTWxhaW1wTW8